SUPPORTING INFORMATION

for

Selective Reduction of Carboxylic Esters Enabled by a Coaxial Double-Tube Continuous-Flow Reactor with On-The-Fly H_2 Degassing

Jiale Wu,[†,‡] Xianjing Zheng,[†,‡] Li Wan,[†,‡] Yuan Tao,[†,‡]

Dang Cheng,*[,†,‡] Fener Chen*[,†,‡]

[†] *Engineering Center for Catalysis and Synthesis of Chiral Molecules, Department of Chemistry, Fudan University, 220 Handan Road, Shanghai 200433, China*

[‡] *Shanghai Engineering & Technology Research Center for Industrial Asymmetric Catalysis of Chiral Drugs, 220 Handan Road, Shanghai 200433, China*

*Corresponding authors:

dcheng@fudan.edu.cn (D. Cheng);

rfchen@fudan.edu.cn (F. E. Chen)

Table of Contents

1 Materials and analytics

All chemical reagents and solvents, unless otherwise specified, were used as obtained from commercial sources without further purification. Tetrahydrofuran (THF) and 1,2-dichloroethane (DCE) were dried by using vigor solvent purification system VSPS-7 (Vigor Gas Purification Technologies Co., Ltd, China). 2-methyltetrahydrofuran (2-MeTHF) was dried by using molecular sieves (4 Å). The substrates **3a~3j** were prepared according to the protocol described in our previous work.[1, 2 3] Lithium borohydride ($LiBH_4$) employed in this work was freshly prepared according to the protocol reported by Brown et al.[4] Analytical thin layer chromatography (TLC) was performed on Silica Gel 60 F_{254} plates under UV light (254 nm). Flash chromatography was performed using Silica Gel 60 (230-400 mesh, Qingdao Haiyang Chemical Co., Ltd, China). ^1H (400 MHz) and ^{13}C NMR (100 MHz) spectra were recorded on a Bruker Avance 400 instrument (Germany) in $CDCl_3$ or DMSO-d_6 at ambient temperature. The chemical shifts are given in δ (ppm) units relative to tetramethylsilane (TMS). Coupling constants (J) are given in hertz (Hz). The multiplicity of a signal is given as: s - singlet; d - doublet; t - triplet; q - quartet; br - broad; m - multiplet. HRMS was analyzed by the Bruker micrOTOF spectrometer. Melting points were measured on a MP450 digital melting point apparatus (Hanon Advanced Technology Group Co., Ltd, China). Optical rotations were determined on a Rudolph AUTOPOL I Automatic Polarimeter (USA). The inline FTIR analysis was performed using the Mettler Toledo ReactIR 702L system (Switzerland). Gas chromatography-mass spectrometry (GC-MS) was performed on an Agilent 5977B GC (HP-5MS column, USA) with an Agilent 7830A MSD. Liquid

chromatography-mass spectrometry (LC-MS) analysis was performed on an Agilent 1260 LC/Q-TOF system (USA) using a EclipsePlusC18 RRHD column (50 mm × 2.1 mm × 1.8 μm) with the mobile phase consisting of MeCN/water (85: 15~90:10, v/v) at a flow rate of 0.5 mL/min. The enantiomeric excess (i.e., ee) was analyzed at 30 ℃ on an Agilent 1220 Infinity II liquid chromatography system equipped with a CHLRALCEL OD-H column (250 mm × 4.6 mm × 5 μm) with the mobile phase consisting of *i*-PrOH/*n*-hexane (70/30, v/v) at a flow rate of 0.5 mL/min. The HPLC analysis was performed on an Agilent 1260 HPLC system (USA) with UV using a EclipsePlus C18 column (50 mm × 2.1 mm × 1.8 μm) with the mobile phase consisting of MeCN/water (85:15~90:10, v/v) at a flow rate of 0.5 mL/min.

2 General procedures for batch reactions

2.1 Reductions of aliphatic unsaturated and polysubstituted aromatic esters

To a stirred solution of the substrate in PhOMe (1.0 M, 0.5 ml) at 0℃ was added dropwise a solution of $LiBH_4$ in PhOMe (1.0 M, 0.75 ml) over a period of 5~10 min. The resulting reaction mixture was then stirred at 45~154 ºC for further reaction. The reaction was constantly monitored by TLC or GC-MS analyses. When the reaction was completed, the reaction mixture was quenched by adding water (5 ml) and extracted three times with extraction solvent (3×10 mL ethyl acetate). The combined organic layers were washed with brine, dried over anhydrous Na_2SO_4 and filtered. The filtrate was concentrated using rotary evaporation under reduced pressure to give product as a white solid or colorless liquid or yellow liquid.

2.2 Reductions of (4*S*, 5*R*)-hemiesters

To a stirred solution of the substrate in THF (0.2 M, 3 ml) at 0 ℃ was added dropwise a solution of $LiBH_4$ in THF (1.0 M, 0.9~1.2 ml) over a period of 5~10 min. The resulting reaction mixture was stirred for 15~30 min after addition and then heated to a higher temperature (45~65 ℃) for further reaction. The reaction was constantly monitored by TLC or LC-MS or GC-MS analyses. As the reduction product (4*S*, 5*R*)-hydroxyl acid **4** is unstable, making it difficult to isolate **4** from the reaction mixture. Therefore, when full conversion of the corresponding substrate was achieved, HCl aqueous solution (1.5 M, 4 ml) was then added, and the resultant reaction mixture was stirred for anther period of time (0.5~1 h) at 60~65 ℃ to effect lactonization. Upon completion of the lactonization reaction, the reaction mixture was extracted three times with extraction solvent (3×5 mL ethyl acetate). The combined organic layers were washed with brine, dried over anhydrous Na_2SO_4, and filtered. The filtrate was concentrated using rotary evaporation under reduced pressure to give product **5** as a white solid. Purification via recrystallization from isopropanol afforded white powder with >99% purity by HPLC analysis.

Table S1. Batch reduction of the model chiral substrate (4*S*, 5*R*)-methyl hemiester with $LiBH_4$ [a]

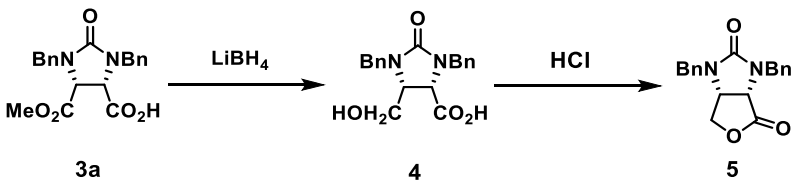

3a 4 5

Entry	Reductant	T (°C)	Molar ratio [b]	Reaction Time (h)	Conv. (%) [c]	Yield (%) [d]	*ee* (%)
1	$LiBH_4$	55	1:1.5	12	100	94	84
2	$LiBH_4$	65	1:1.5	12	100	94	82.5

[a] Reaction conditions: the reaction was carried out on a 0.6 mmol scale. [b] The molar ratio of substrate/reductant. [c] Conversion of the substrate was determined by liquid chromatography-mass spectrometry (LC-MS) analysis. [d] The reduction product (4*S*, 5*R*)-hydroxyl acid **4** is unstable, making it difficult to obtain its isolated yield; hence the lactonization was effected by adding 1.5 M HCl aqueous solution (4 ml) into the reaction mixture upon completion of the reduction reaction to obtain the isolated yield of the product (3a*S*, 6a*R*)-lactone **5**.

3. General procedures for flow reactions

3.1 The normal flow system

The normal flow system composed of two pumps (P1, P2, Fusion 4000, Chemyx, USA), two check valves (CV, IDEX Health & Science, USA), a PTFE (polytetrafluoroethylene) T-shaped micromixer (M, 0.8 mm i.d., Nanjing Runze Fluid Control Equipment Co., LTD., China), a coil reactor of perfluoroalkoxy alkane (PFA) tube (0.8 mm i.d., 1.6 mm o.d., Nanjing Runze Fluid Control Equipment Co., LTD., China) and a back pressure regulator (BPR, IDEX Health & Science, USA) was constructed as shown in Figure S1. The coil reactor was immersed in an oil bath (IKA RCT basic, Germany) to ensure the required reaction temperature.

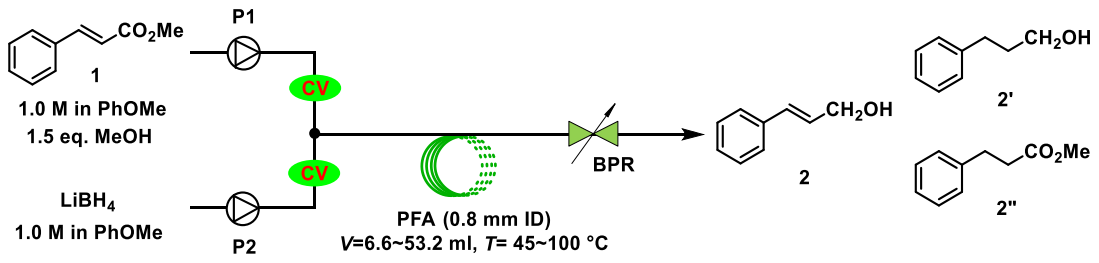

Figure S1. The normal flow system for the $LiBH_4$ mediated reductions.

A solution of the substrate in PhOMe (1.0 M) with 1.5 equivalents of MeOH and a solution of $LiBH_4$ in PhOMe (1.0 M) were introduced into the T-shaped micromixer at the desired flow rates, respectively. The two solutions were mixed via the T-shaped micromixer and then the combined reaction mixture was streamed through the coil reactor at a preset temperature (45~100 ℃). The reaction solution left the flow system through the back pressure regulator. As mixing between the substrate solution and $LiBH_4$ solution led to the formation of hydrogen gas, which affected the actual flow velocity of the reaction mixture in the coil reactor, so the length of the coil reactor (i.e., reaction volume) was varied to ensure the desired residence time of the reaction mixture (Table S2). The flow rates of the substrate solution and $LiBH_4$ solution were listed in Table S2. The actual residence time (t_R) of the reaction mixture was in the range of 2.5~20 min.

Table S2. Operating conditions employed in the normal flow system [a]

Entry	t_R (min) [b]	Pump flow rate of substrate solution (P1, ml/min) [c]	Pump flow rate of $LiBH_4$ solution (P2, ml/min) [d]	V (ml) [e]	T (℃) [f]	P (bar) [g]
1	2.5	0.3	0.45	6.6	45	1.0
2	5	0.3	0.45	13.4	45	1.0
3	7.5	0.3	0.45	20.0	45	1.0
4	10	0.3	0.45	26.5	45	1.0
5	20	0.3	0.45	53.2	45	1.0
6	5	0.3	0.45	13.4	70	1.0
7	10	0.3	0.45	20.0	70	1.0
8	5	0.3	0.45	13.4	70	2.5
9	5	0.3	0.45	13.4	70	5.0

10	5	0.3	0.45	13.4	70	7.0
11	5	0.3	0.45	13.4	80	5.0
12	5	0.3	0.45	13.4	90	5.0
13	5	0.3	0.45	13.4	100	5.0

[a] The molar ratio of substrate/$LiBH_4$/MeOH was 1:1.5:1.5. [b] The actual residence time of the reaction mixture through the coil reactor. [c] The flow rate of the pump P1. [d] The flow rate of the pump P2. [e] The reaction volume (*V*) of the coil reactor was varied by changing its length. [f] The temperature of the coil reactor. [g] Back pressure value.

3.2 The coaxial double-tube reactor based flow system

The coaxial double-tube continuous-flow reactor prototype consisted of an inner tube (PFA, 1.6 mm o.d. and 0.8 mm i.d.) and an outer tube (PFA, 6.35 mm o.d. and 4.75 mm i.d.). It was constructed in-house from commercially available components (Table S3) including PFA tubes (perfluoroalkoxy alkane), stainless steel fittings and PTFE (polytetrafluoroethylene) fittings.

Table S3. Components used for the contruction of the coaxial double-tube reactor

①	PTFE straight connector, 1/4"-28 (1/6" tubing) × 1/4"-28 (1/8" tubing)
②	stainless steel connector, 1/4” (6.35 mm) × 1/8” (3.17 mm) tube o.d.
③	stainless steel union tee, 1/4” (6.35 mm) tube o.d.
④	stainless steel union tee, 1/4” (6.35 mm) tube o.d.
⑤	stainless steel connector, 1/4” (6.35 mm) × 1/16” (1.6 mm) tube o.d.
⑥	PFA tubing 1/16” (1.6 mm) o.d. × 0.031” (0.8 mm) i.d.
⑦	PFA tubing 1/8” (3.17 mm) o.d. × 0.08” (2.03 mm) i.d.
⑧	PFA tubing 1/4” (6.35 mm) o.d. × 3/16” (4.75 mm) i.d.

As shown in Figure S2, the outer tube ⑧ was composed of three segments (i.e., ⑧-①, ⑧-② and ⑧-③), segment ⑧-① was connected with segment ⑧-② via the stainless steel

union tee ③, and segment ⑧-2 was connected with segment ⑧-3 via the stainless steel union tee ④. The top end of segment ⑧-1 was connected with tube ⑦ via the stainless steel connector ②. The inner tube ⑥ passed through the PTFE straight connector ①, the stainless steel connector ②, the stainless steel union tee ③ and the stainless steel union tee ④, and protruded 30 mm from the stainless steel union tee ③ inside the outer tube ⑧-2. A PFA coil (0.8 mm i.d., 1.6 mm o.d., 3.76 ml of residence volume) was connected to the bottom of the outer tube ⑧-3 via stainless steel connector ⑤. This coaxial double-tube reactor was installed vertically. Note that the inner tube did not completely go through the outer tube but only protruded inside the outer tube. The outlet of the inner tube was located below the gas outlet. Both the gas inlet and outlet were connected to the outer tube. The gas inlet was connected to a nitrogen gas supply via a gas mass flow meter, and the pressure of the inlet nitrogen gas can be accurately adjusted. The gas outlet was connected to a fume hood.

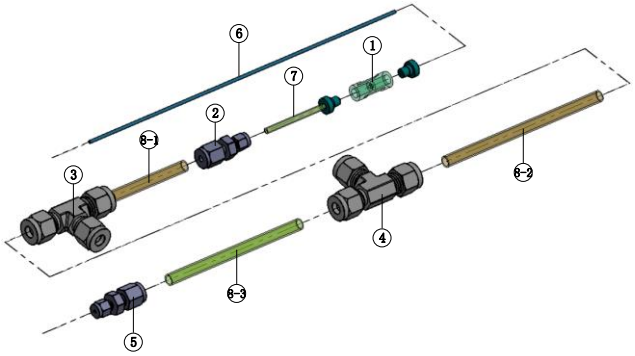

(a)

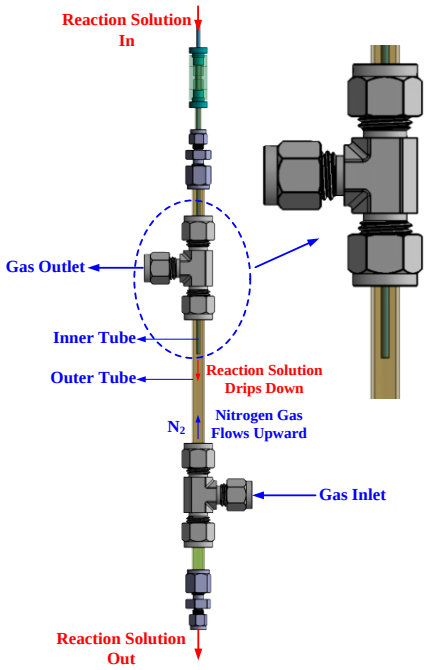

(b)

Figure S2. Expanded (a) and assembled (b) diagrams of the coaxial double-tube continuous-flow reactor.

As shown in Figure S3, the coaxial double-tube flow system was composed of three pumps (P3, P4: HPLC pump AP0010, Sanotac, China; P5: peristaltic pump, Model 77200-60, Masterflex, Germany), two check valves (CV, IDEX Health & Science, USA), a PTFE (polytetrafluoroethylene) T-shaped micromixer (M, 0.8 mm i.d., Nanjing Runze Fluid Control Equipment Co., LTD., China), one coaxial double-tube reactor, and a coil reactor of perfluoroalkoxy alkane (PFA) tube (0.8 mm i.d., 1.6 mm o.d., 3.76 ml of residence volume, Nanjing Runze Fluid Control Equipment Co., LTD., China). The coil reactor was immersed in an oil bath (IKA RCT basic, Germany) to ensure the required reaction temperature.

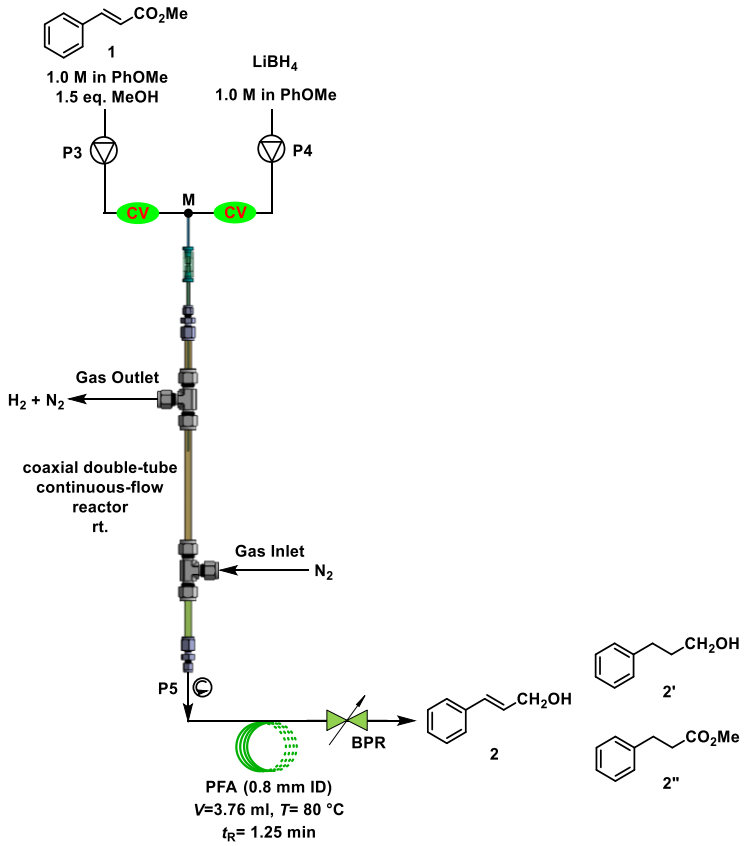

Figure S3. The coaxial double-tube reactor based continuous-flow system.

In the coaxial double-tube flow system, the top end of the inner tube was connected to the T-shaped micromixer (0.8 mm i.d.), whereby a substrate solution and a $LiBH_4$ solution were mixed at the desired flow rates, respectively, and the resulting mixture was introduced into the outer tube from its top end via the inner tube. In the meantime, nitrogen gas was introduced into the outer tube from the gas inlet located at its bottom end. In this way, the reaction solution dripped down while the nitrogen gas flowed upward in this coaxial double-tube reactor. Hence the generated hydrogen gas was removed on-the-fly from the reaction solution facilitated by the upflowing nitrogen gas, and the off-gas (i.e., nitrogen gas and the generated hydrogen gas) was discharged from the gas outlet. The gas flow rate and pressure of the input nitrogen gas needs to be operated within 5~120 ml/min and 1.0~7.0 bar, respectively, as larger flow rate or pressure of the input nitrogen gas would easily lead to flooding.

When the reaction solution reached the bottom of the outer tube, it was then streamed through the downstream coil reactor driven by a peristaltic pump (P5). The coaxial double-tube reactor was placed at room temperature and the downstream coil reactor was immersed in an oil bath (IKA RCT basic, Germany) to ensure the required reaction temperature (25~100 ^{o}C).

To reduce methyl cinnamate, a solution of methyl cinnamate in anisole (1.0 M) with 1.5 equivalents of MeOH and a solution of $LiBH_4$ in anisole (1.0 M) were introduced into the coaxial double-tube reactor at the desired flow rates, respectively, via the T-type micromixer (M, 0.8 mm i.d.). The operating conditions were listed in Table S4.

Table S4. Operating conditions employed in the coaxial double-tube flow reduction of the model substrate methyl cinnamate [a]

Entry	t_R (min) [b]	T (°C) [c]	P (bar) [d]	Pump flow rate of substrate solution (P3, ml/min) [e]	Pump flow rate of $LiBH_4$ solution (P4, ml/min) [f]	Pump flow rate of mixed reaction solution (P5, ml/min) [g]
1	5	50	2.5	0.3	0.45	0.75
2	7.5	50	2.5	0.2	0.3	0.50
3	10	50	2.5	0.15	0.23	0.38
4	5	60	2.5	0.3	0.45	0.75
5	5	70	2.5	0.3	0.45	0.75
6	5	80	2.5	0.3	0.45	0.75
7	5	90	2.5	0.3	0.45	0.75
8	2.5	80	2.5	0.6	0.9	1.5
9	1.25	80	2.5	1.2	1.8	3.0

[a] The molar ratio of substrate/$LiBH_4$/MeOH was controlled at 1:1.5:1.5. [b] The residence time of the reaction mixture through the flow system. [f] The temperature of the coil reactor. [c] Back pressure value. [d] The flow rate of the pump P3. [e] The flow rate of the pump P4. [f] The flow rate of the pump P5.

To obtain the isolated yields given in the Table 4, the following workup procedure was adopted: 10 ml reaction solution was collected in a vial that was pre-filled with 10 ml water. This mixture was then extracted three times with extraction solvent (3×10 mL ethyl acetate). The combined organic layers were washed with brine, dried over anhydrous Na_2SO_4 and filtered. The filtrate was concentrated using rotary evaporation under reduced pressure to give crude product. The crude product was purified by flash column chromatography on silica gel (petroleum ether/ethyl acetate 8:1, v/v) to afford the pure product.

To reduce (4*S*, 5*R*)-methyl hemiester, a solution of (4*S*, 5*R*)-methyl hemiester in THF (0.8 M) and a solution of $LiBH_4$ in anisole (1.0 M) were introduced into the coaxial double-tube reactor at 0.684 ml/min (P3) and 0.821 ml/min (P4), respectively, via the T-type micromixer (M, 0.8 mm i.d.). The flow rate of the peristaltic pump (P5) was set at 1.50 ml/min (Figure S4).

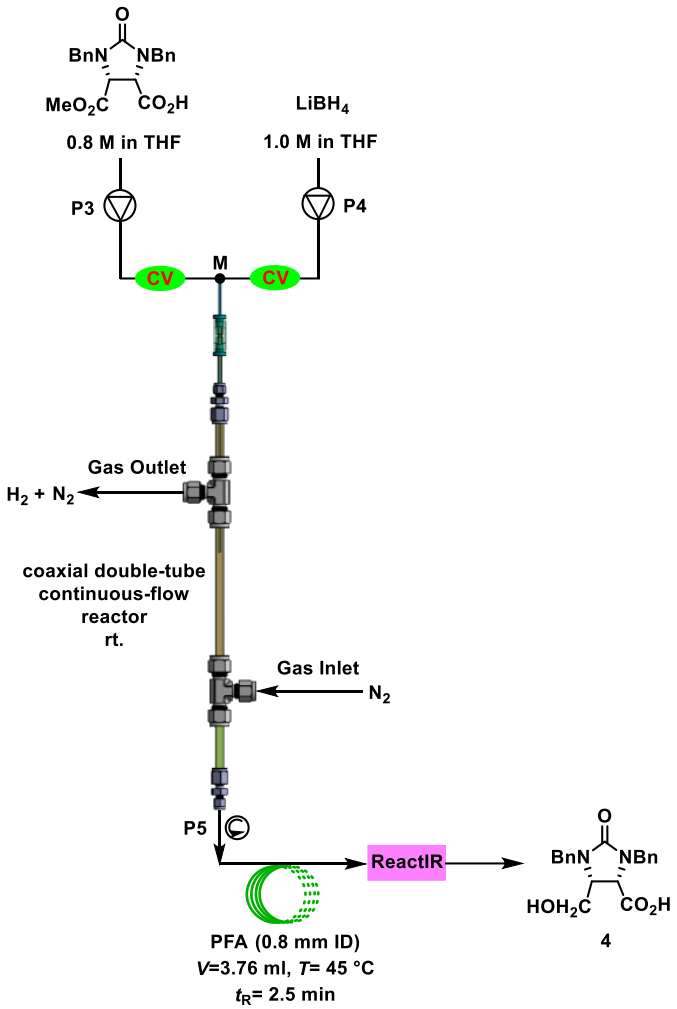

Figure S4. The coaxial double-tube reactor based continuous-flow system for the reduction of (4*S*, 5*R*)-hemiesters.

4 Inline FTIR monitoring

As shown in Figure S4, the inline FTIR ReactIR 702L (Mettler Toledo, Switzerland)

was coupled with the flow reactor via the bespoke micro flow cell with an internal volume of 50 μL. The attenuated total reflectance (ATR) sensor was integrated into the ReactIR flow cell, which allows *in situ*, real-time analysis and monitoring of chemical reactions.[5] The FTIR spectra were recorded and analyzed with iC-IR analysis software (Mettler Toledo, Switzerland). Reference spectra of (4*S*, 5*R*)-methyl hemiester, THF and $LiBH_4$ were recorded (Figures S5 and S6), respectively, in order to analyze the reaction process. Analysis of the FTIR spectra shown in Figure S5 revealed two peaks at 1718 cm^{-1} and 1754 cm^{-1} for the two carbonyl groups of the carboxylic and carboxylic ester groups, respectively (Figures S5 and S6). As expected, the band at 1718 cm^{-1} shifted to 1700 cm^{-1} and the band at 1754 cm^{-1} reduced in intensity as the reduction reaction proceeded, while a band at 1592 cm^{-1} corresponding to the formed hydroxyl group was observed (Figure S6).

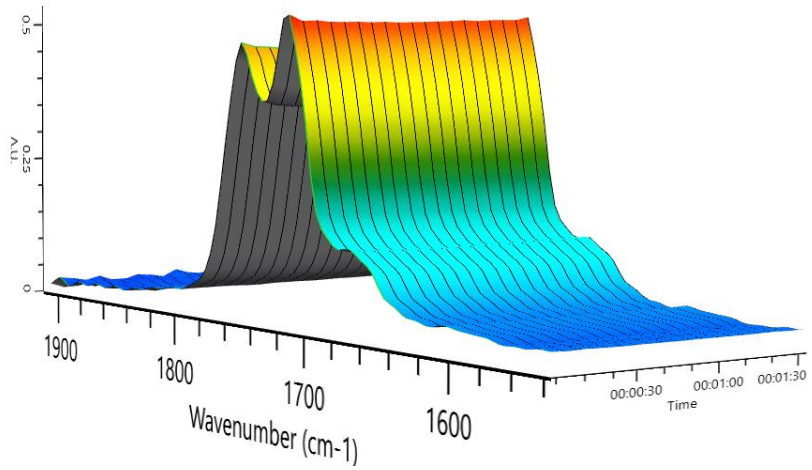

Figure S5. Three-dimensional time-resolved spectral data of the neat (4*S*, 5*R*)-methyl hemiester.

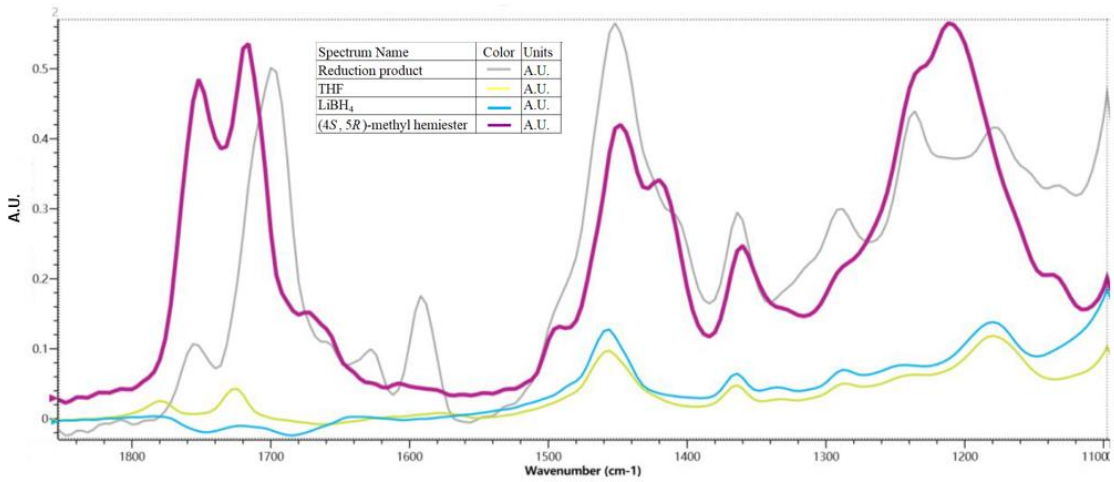

Figure S6. FTIR spectra of the (4*S*, 5*R*)-methyl hemiester, $LiBH_4$, solvents and $LiBH_4$ (gray line: reduction product; yellow line: THF; blue line: $LiBH_4$; purple line: (4*S*, 5*R*)-methyl hemiester).

Calibration of the FTIR spectrometer for quantitative analysis was carried out by analyzing a series of solutions of known concentrations of the substrate (4*S*, 5*R*)-methyl hemiester. As shown in Figure S7, a good linearity between the intensity of the 1754 cm^{-1} absorption band and the concentration of the substrate was observed. Thus, conversions can be readily quantified during the continuous flow reductions, enabling rapid reaction optimizations in flow.

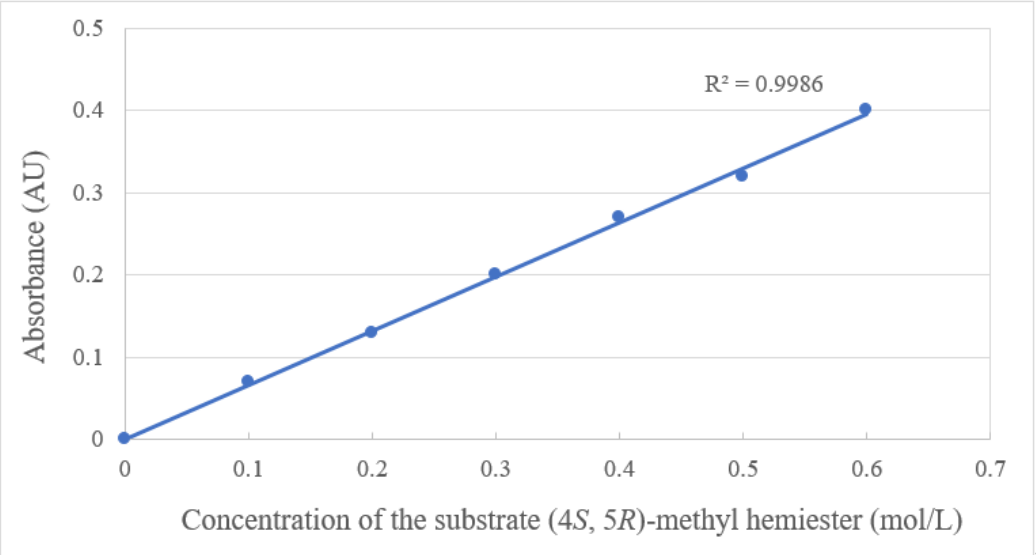

Figure S7. Intensity of the 1754 cm^{-1} absorption band as a function of the concentration of the substrate.

5 Optimization of the lactonization-extraction step in flow

P6 (HPLC pump, AP0010, Sanotac, China) was used to pump the reaction solution from step I that was collected in a container, P7 (HPLC pump, AP0010, Sanotac, China) was used to pump the HCl aqueous solution (1.5 M), and P8 (HPLC pump, AP0010, Sanotac, China) was employed to pump the extraction solvent.

Table S5. Optimization of the lactonization-extraction step in flow

Entry	Flow rate of reaction solution (P6, ml/min)	Flow rate of HCl aq. solution (P7, ml/min)	Flow rate of extraction solvent (P8, ml/min)	t_R (min) [f]	V_2 (ml) [g]	T (°C) [h]	Conv. (%) [I]
1	0.11	0.11	0.22 [a]	0.7	3.76	60	81.0
2	0.11	0.11	0.22 [a]	1.2	5.01	60	83.6
3	0.11	0.11	0.22 [a]	1.8	7.52	60	86.2
4	0.11	0.11	0.22 [a]	3.5	15.04	60	86.1
5	0.11	0.11	0.22 [a]	5.5	25.04	60	87.0
6	0.11	0.11	0.22 [a]	1.8	7.52	65	96.3

7	0.11	0.11	0.22 [a]	1.5	7.52	70	100
8	0.11	0.11	0.16 [a]	2.2	7.52	70	100
9	0.11	0.11	0.10 [a]	2.7	7.52	70	100
10	0.11	0.11	0.10 [b]	2.7	7.52	70	100
11	0.11	0.11	0.10 [c]	2.7	7.52	70	100
12	0.11	0.11	0.10 [d]	2.7	7.52	70	100
13	0.11	0.11	0.10 [e]	2.7	7.52	70	100

[a] The extraction solvent was EtOAc. [b] The extraction solvent was 2-MeTHF. [c] The extraction solvent was *i*-PrOAc. [d] The extraction solvent was PhMe. [e] The extraction solvent was DCE. [f] The actual residence time of the reaction mixture through reactor II. The contact between reaction solution from step I and HCl aqueous solution still led to the formation of hydrogen gas due to the presence of excess $LiBH_4$, which affected the actual flow velocity of the reaction mixture in reactor II. [g] The internal volume of reactor II (V_2) was varied by changing its length. [h] The temperature of reactor II. [I] Conversion of the substrate was determined by liquid chromatography-mass spectrometry (LC-MS) analysis.

6 Liquid-liquid membrane separator

The liquid-liquid membrane separator (LLMS) was composed of two stainless steel plates (160 mm × 30 mm × 10 mm). There was a separating channel of 0.8 mm (width) × 0.6 mm (depth) × 120 mm (length) on each of the two plates. A piece of 0.45 μm pore hydrophobic PTFE membrane (Pall Zeflour, USA) was sandwiched between the two plates to divide the two separating channels. The aqueous-organic phase separation was realized when the liquid-liquid biphasic mixture flowing through one of the two separating channels, which was enabled by the hydrophobic PTFE membrane. The inlet and outlets (1/4"-28 standard flat-bottom port) were connected with the separating channels via 0.5 mm thru holes. The fluidic connections were realized by means of standard 1/4"-28 thread fittings with 1/16" tubing. The photo of the liquid-liquid membrane-based microseparator used in this work is presented in Figure S8.

Figure S8. Photo of the liquid-liquid membrane separator.

7 Micromixers

The use of T-type micromixers was found to have provided satisfactory mixing for miscible fluids in the reduction and lactonization steps. However, when two immiscible liquids were involved, the employment of T-type micromixer led to an unsatisfactory mixing of the two streams. Therefore, a two-phase cross-flow micromixer (CFMM) was employed as M3 to mix the reaction solution with the extraction solvent in the lactonization-extraction synergized process (i.e., the immiscible liquid-liquid system). As shown in Figure S9, the in-house manufactured CFMM comprised two parallel microchannels (microchannel A of 0.8 mm×0.5 mm×25 mm and microchannel B of 0.8 mm×0.5 mm×15 mm); Inlet 1 was connected with microchannel A, Inlet 2 was connected with microchannel B, and the Outlet was connected with microchannel A; Inlet 1 and Inlet 2 were arranged at the same side; there was an apertured section with 50 μm micropores in the wall shared by microchannel A and microchannel B.

In setting up the lactonization-extraction synergized process, the extraction solvent (e.g.,

EtOAc) was introduced into microchannel A via Inlet 1, while the reaction solution was delivered into microchannel B via Inlet 2; after the microchannel B was filled, the reaction solution flowed through the apertured section into microchannel A to form a biphasic mixture, where the reaction solution was the dispersed phase and the extraction solvent was the continuous phase.

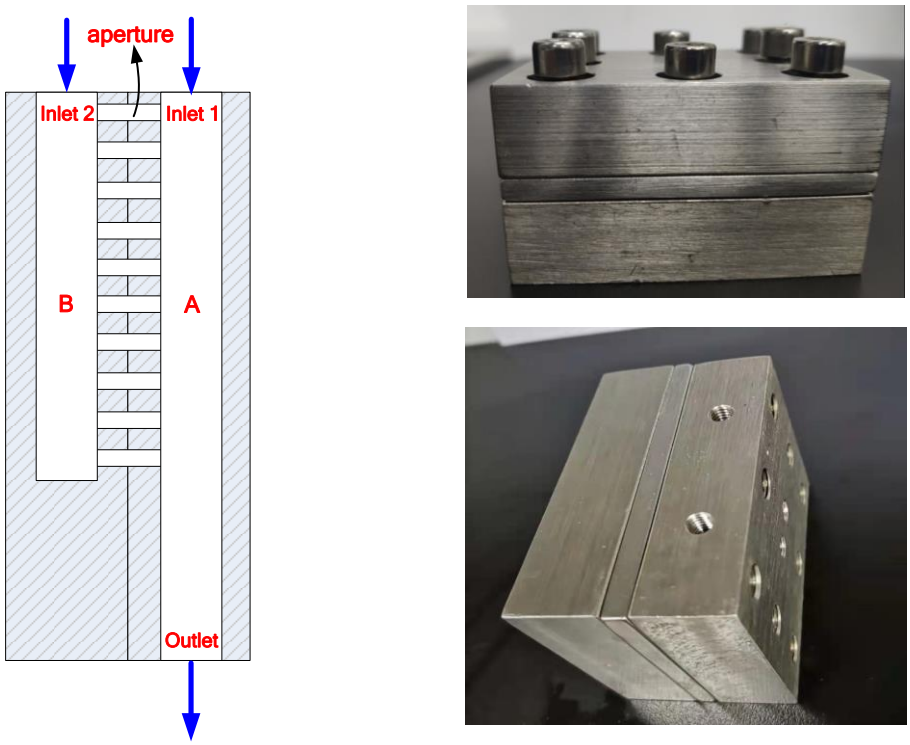

(a) (b)

Figure S9. (a) Schematic illustration of the two-phase cross-flow micromixer (CFMM), (b) photos of the two-phase cross-flow micromixer.

8 Photo of the experimental setup of the coaxial double-tube reactor based continuous-flow system

Figure S10. Photo of the experimental setup of the coaxial double-tube reactor based continuous-flow system.

9 Calculations of Space-Time Yield and Process Mass Intensity

The Space-Time Yield (STY) was calculated according to the following equation:

$$\text{STY} = \frac{\text{Yield [g]}}{\text{Total reactor volume [L]} \times \text{time [h]}} \quad \text{(S1)}$$

where total reactor volume=16.60 ml.

When the flow system was operated constantly for 12 hours, the product obtained was 8.72 g (Entry 1 in Table 7). Therefore, the STY was 43.8 g L^{-1} h^{-1}.

When the flow system was operated constantly for 24 hours, the product obtained was

17.53 g (Entry 2 in Table 7). Therefore, the STY was 44.0 g L^{-1} h^{-1}.

The Process Mass Intensity (PMI) was calculated according to the following equation:

$$\text{PMI} = \frac{\text{Total mass used in the process [g]}}{\text{Mass of product [g]}} \quad \text{(S2)}$$

According to the definition of PMI, water was not included in the calculation of the total mass.[6,7]

When the flow system was operated constantly for 24 hours, the product obtained was 17.53 g (Entry 2 in Table 7), and the total mass used (excluding the extraction solvent) in the process was 161.42 g. Therefore, the PMI was 9.21.

When the flow system was operated constantly for 24 hours, the product obtained was 17.53 g (Entry 2 in Table 7), and the total mass used (including the extraction solvent) in the process was 291.31 g. Therefore, the PMI was 16.62.

10 Analytical data of the reductive products

(*E*)-3-phenylprop-2-en-1-ol

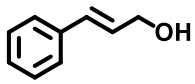

colorless crystalline solid, ***m.p.*** 33.2 – 34.2 ºC, **^{1}H NMR** (400 MHz, $CDCl_3$) δ 7.44 – 7.39 (m, 2H), 7.38 – 7.32 (m, 2H), 7.30 – 7.26 (m, 1H), 6.64 (d, *J* = 16.0 Hz, 1H), 6.42 – 6.35 (m, 1H), 4.34 (dd, *J* = 5.6, 1.6 Hz, 2H), 2.18 (s, 1H); **^{13}C NMR** (100 MHz, $CDCl_3$) δ 136.7, 130.9, 128.6, 128.6, 127.7, 126.5, 63.4; IR: 3414, 3027, 2819, 1501, 1472, 1102, 1022, 746, 711.

(*E*)-3-(4-chlorophenyl)prop-2-en-1-ol

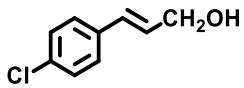

White soild, ***m.p.*** 50.8 – 51.8 ºC, **^{1}H NMR** (400 MHz, $CDCl_3$) δ 7.30 (s, 4H), 6.57 (d, *J* = 16.0 Hz, 1H), 6.37 – 6.31 (m, 1H), 4.33 (d, *J* = 5.2 Hz, 2H), 2.02 (s, 1H);**^{13}C NMR** (100 MHz, $CDCl_3$) δ 135.1, 133.2, 129.7, 129.1, 128.7, 127.6, 63.5; IR: 3304, 3021, 2917, 1578, 1369, 1218, 918, 798, 682.

(*E*)-3-(4-(bromomethyl)phenyl)prop-2-en-1-ol

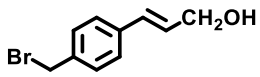

white solid, ***m.p.*** 79.5 – 80.5 ºC, **^{1}H NMR** (400 MHz, $CDCl_3$) δ 7.37 (s, 4H), 6.67 – 6.58 (m, 1H), 6.43 – 6.37 (m, 1H), 4.51 (s, 2H), 4.35 (dd, *J* = 5.6, 1.6 Hz, 2H), 1.73 (s, 1H); **^{13}C NMR** (100 MHz, $CDCl_3$) δ 137.1, 136.9, 130.2, 129.5, 129.4, 126.9, 63.6, 33.5; IR: 3364, 3021, 2913, 1557, 1413, 1359, 1109, 961, 848, 735, 657.

(*E*)-3-(4-bromophenyl)prop-2-en-1-ol

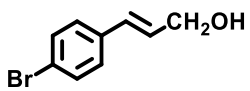

White soild, ***m.p.*** 65.6 – 66.4 ºC, **^{1}H NMR** (400 MHz, $CDCl_3$) δ 7.45 (d, *J* = 8.2 Hz,

2H), 7.26 (d, *J* = 8.2 Hz, 2H), 6.57 (d, *J* = 16.0 Hz, 1H), 6.40 – 6.33 (m, 1H), 4.33 (d, *J* = 5.2 Hz, 2H), 1.77 (s, 1H); **^{13}C NMR** (100 MHz, $CDCl_3$) δ 135.6, 131.7, 129.8, 129.3, 128.0, 121.4, 63.5; IR: 3394, 2978, 2803, 1541, 1399, 1225, 1042, 846, 746.

(*E*)-3-(p-tolyl)prop-2-en-1-ol

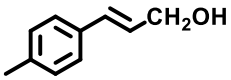

Colorless solid, ***m.p.*** 51.2 – 52.3 ºC, **^{1}H NMR** (400 MHz, $CDCl_3$) δ 7.31 (d, *J* = 8.0 Hz, 2H), 7.15 (t, *J* = 8.4 Hz, 2H), 6.60 (d, *J* = 16.0 Hz, 1H), 6.38 – 6.31 (m, 1H), 4.33 (d, *J* = 5.6 Hz, 2H), 2.37 (s, 3H); 1.83 (s, 1H); **^{13}C NMR** (100 MHz, $CDCl_3$) δ 137.6, 133.9, 131.2, 129.3, 127.4, 126.4, 63.8, 21.2, IR: 3414, 3319, 3021, 2873, 1536, 1379, 1082, 981, 746, 691.

3-phenylprop-2-yn-1-ol

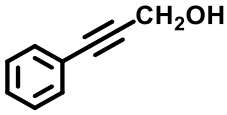

Light yellow oil; **^{1}H NMR** (400 MHz, $CDCl_3$) δ 7.46 (s, 2H), 7.34 (s, 3H), 4.52 (s, 2H); 2.05 (s, 1H); **^{13}C NMR** (100 MHz, $CDCl_3$) δ 131.7, 128.5, 128.3, 122.5, 87.2, 85.7, 51.7; IR: 3340, 2889, 1578, 1478, 1431, 1053, 914, 753, 681, 522.

Omega-Undecylenyl alcohol

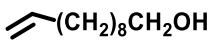

colorless liquid; **^{1}H NMR** (400 MHz, $CDCl_3$) δ 5.85 – 5.75 (m, 1H), 5.03 – 4.87 (m, 2H), 3.62 (t, *J* = 6.7 Hz, 2H), 2.03 (dd, *J* = 14.4, 6.8 Hz, 2H), 1.62 – 1.47 (m, 3H), 1.40 – 1.27 (m, 12H); **^{13}C NMR** (100 MHz, $CDCl_3$) δ 139.1, 114.1, 62.8, 33.8, 32.7, 29.5, 29.4, 29.1, 28.9, 25.7; IR: 3452, 2929, 1621, 1423, 1033, 891.

(4-ethynylphenyl)methanol

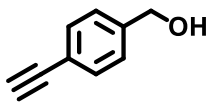

yellow oil, ^{1}H NMR (400 MHz, $CDCl_3$) δ 7.49 (d, J = 8.2 Hz, 2H), 7.30 (d, J = 8.2 Hz, 2H), 4.67 (s, 2H), 3.10 (s, 1H), 2.51 (s, 1H); ^{13}C NMR (100 MHz, $CDCl_3$) δ 141.6, 132.3, 126.8, 121.2, 83.5, 77.3, 64.7; IR: 3290, 2869, 1494, 1429, 1207, 998, 813, 633.

(4-chlorophenyl)methanol

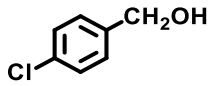

colorless crystal, ***m.p.*** 69.3 – 70.1 °C; **^{1}H NMR** (400 MHz, $CDCl_3$) δ 7.33 – 7.28 (m, 2H), 7.24 (d, J = 8.3 Hz, 2H), 4.58 (s, 2H); **^{13}C NMR** (100 MHz, $CDCl_3$) δ 139.2, 133.2, 128.6, 128.2, 64.0; IR: 3352, 2902, 1629, 1492, 1108, 1024, 744, 721.

(4-bromophenyl)methanol

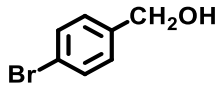

crystalline powder, ***m.p.*** 75.5 – 76.3 °C; **^{1}H NMR** (400 MHz, $CDCl_3$) δ 7.46 (d, J = 8.4 Hz, 2H), 7.19 (d, J = 8.4 Hz, 2H), 4.59 (d, J = 4.9 Hz, 2H), 2.33 (t, J = 5.3 Hz, 1H); **^{13}C NMR** (100 MHz, $CDCl_3$) δ 139.7, 131.6, 128.6, 121.4, 64.4; IR:3429, 1524, 1138, 1013, 788.

(4-nitrophenyl)methanol

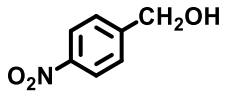

white soild, ***m.p.*** 78.4 – 79.1 °C; **^{1}H NMR** (400 MHz, $CDCl_3$) δ 8.18 (d, J = 8.4 Hz, 2H), 7.51 (d, J = 8.4 Hz, 2H), 4.72 (s, 2H), 2.38 (s, 1H); **^{13}C NMR** (100 MHz, $CDCl_3$) δ 147.6, 146.5, 126.3, 123.1, 63.3; IR:3321, 1621, 1414, 1325, 1123, 1075, 804.

(3-chlorophenyl)methanol

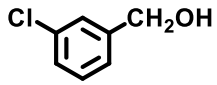

colorless liquid; **^{1}H NMR** (400 MHz, $CDCl_3$) δ 7.34 – 7.21 (m, 3H), 7.21 – 7.11 (m, 1H), 4.56 (s, 2H), 3.40 (s, 1H); **^{13}C NMR** (100 MHz, $CDCl_3$) δ 142.8, 134.3, 129.8, 127.6, 126.9, 124.9, 64.1; **IR** 3424, 2989, 1556, 1432, 1200, 1036, 787, 689.

(2-chlorophenyl)methanol

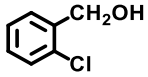

white crystalline powder, ***m.p.*** 69.2-70.0 ºC; **^{1}H NMR** (400 MHz, $CDCl_3$) δ 7.46 (dd, *J* = 7.4, 1.7 Hz, 1H), 7.36 (dd, *J* = 7.5, 1.6 Hz, 1H), 7.31 – 7.20 (m, 2H), 4.74 (s, 2H), 2.97 (s, 1H); **^{13}C NMR** (100 MHz, $CDCl_3$) δ 138.1, 132.6, 129.3, 128.7, 128.6, 127.0, 62.5; **IR** 3421, 3202, 1456, 1054, 1039, 1019, 741.

(3a*S*,6a*R*)-1,3-dibenzyltetrahydro-1*H*-furo[3,4-*d*]imidazole-2,4-dione 5

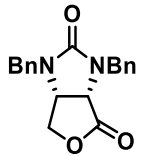

white solid; ***m.p.*** 119.3 – 120.1 ℃; $[\alpha]_D^{25}$ = +61.2 (c 2.0, $CHCl_3$); **^{1}H NMR** (400 MHz, $CDCl_3$) δ 7.50 – 7.23 (m, 10H), 5.05 (d, *J* = 14.8 Hz, 1H), 4.64 (d, *J* = 15.2 Hz, 1H), 4.38 (dd, *J* = 15.2, 10.4 Hz, 2H), 4.24 – 4.08 (m, 3H), 3.94 (d, *J* = 8.6 Hz, 1H); **^{13}C NMR** (100 MHz, $CDCl_3$) δ 172.9, 158.2, 136.0, 135.9, 129.0, 128.8, 128.2, 128.1, 127.9, 70.1, 54.4, 52.5, 46.9, 45.2; IR: 3064, 1704, 1264,1220, 728 cm^{-1}; $[M+Na]^+$ calcd for $C_{19}H_{18}N_2NaO_3$ 345.1210, found 345.1211.

11 ^{1}H NMR and ^{13}C NMR spectra of the reductive products

(*E*)-3-phenylprop-2-en-1-ol

^{1}H NMR

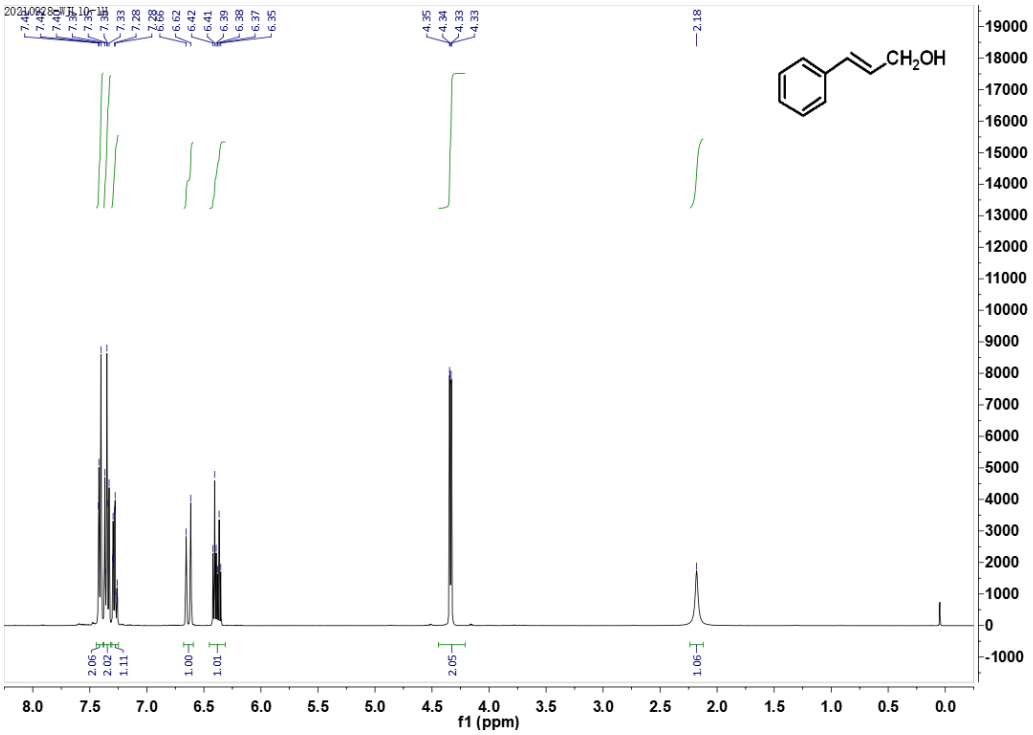

^{13}C NMR

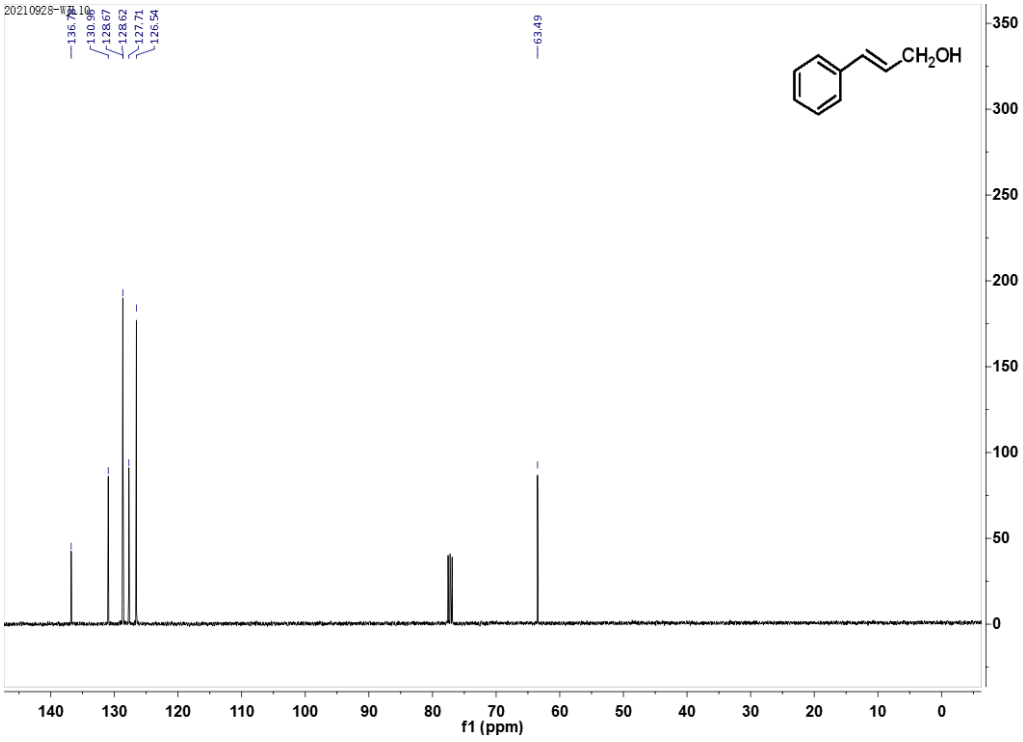

(*E*)-3-(4-chlorophenyl)prop-2-en-1-ol

^{1}H NMR

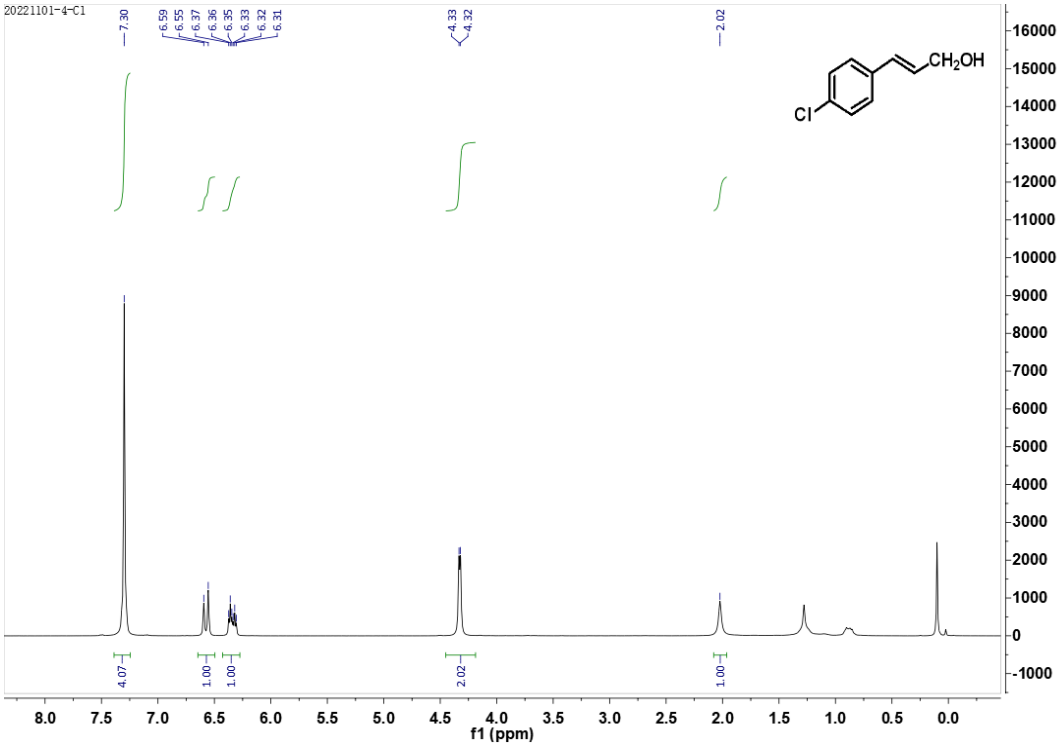

^{13}C NMR

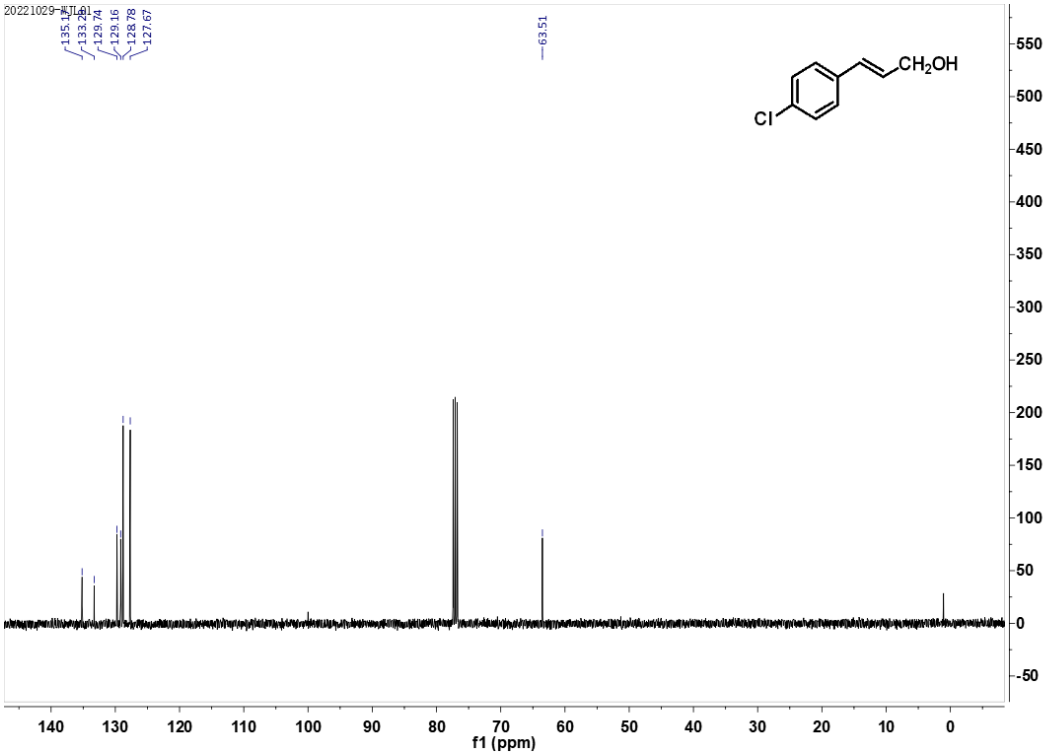

(*E*)-3-(4-(bromomethyl)phenyl)prop-2-en-1-ol

^{1}H NMR

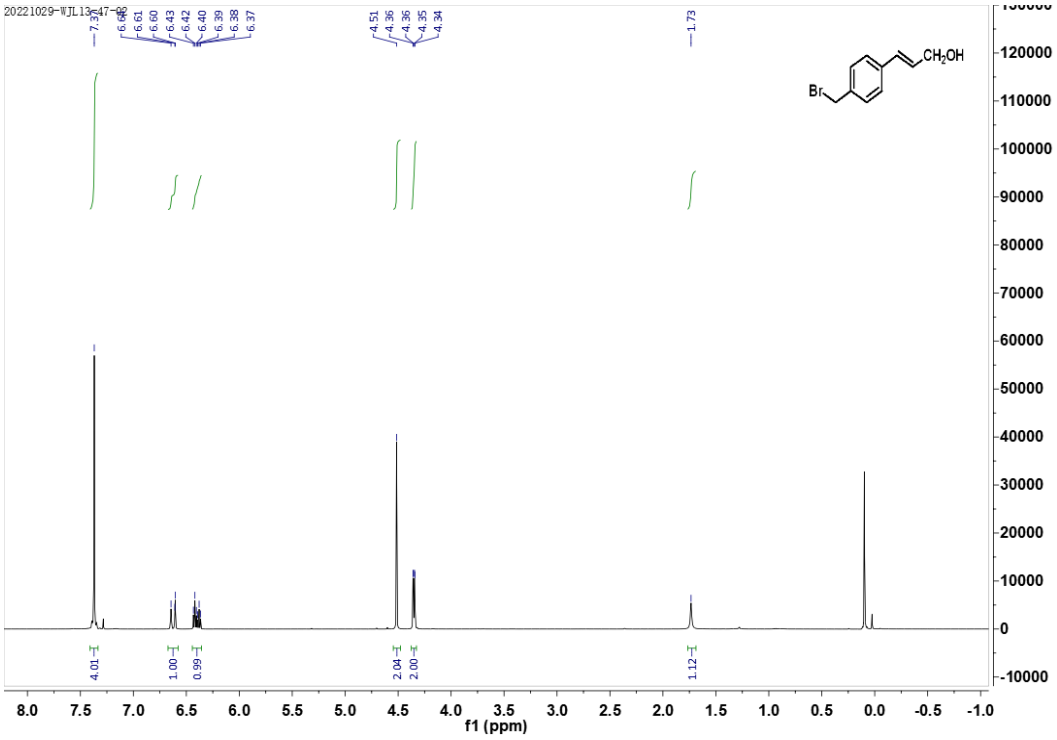

^{13}C NMR

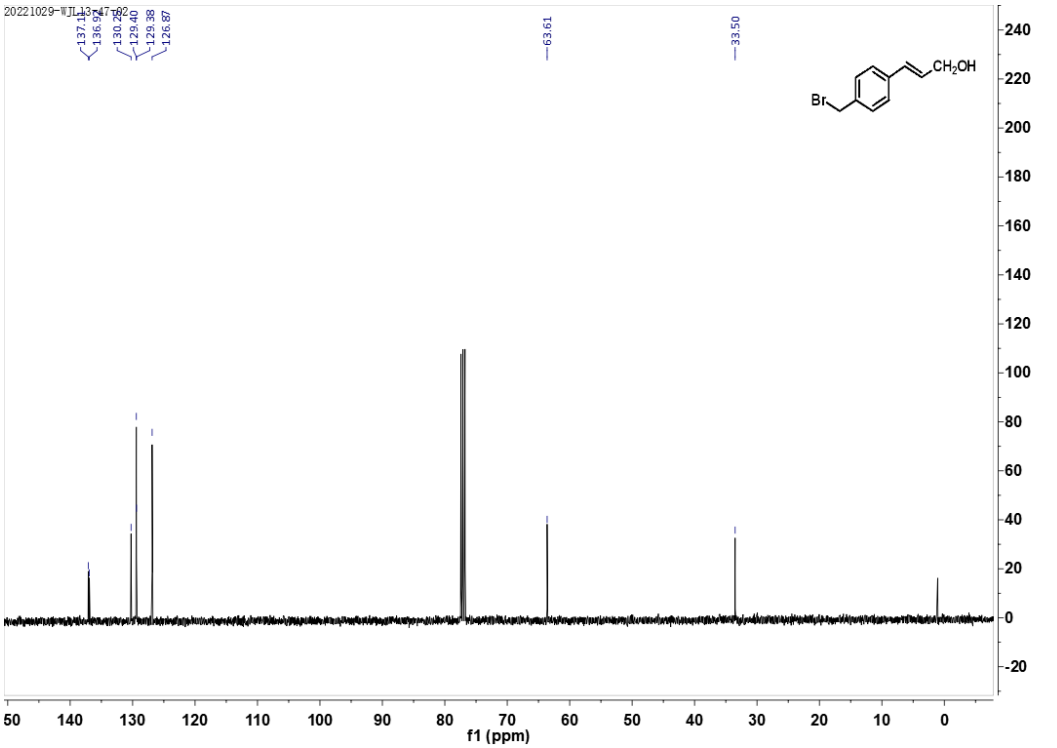

(*E*)-3-(4-bromophenyl)prop-2-en-1-ol

^{1}H NMR

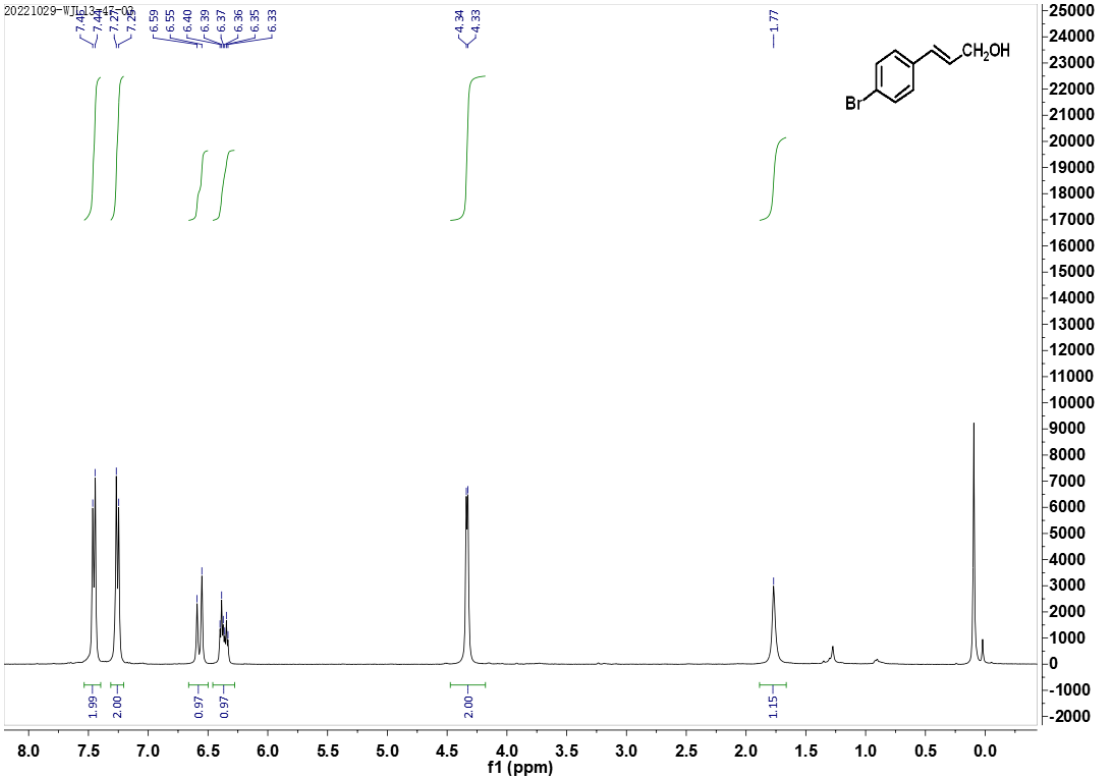

^{13}C NMR

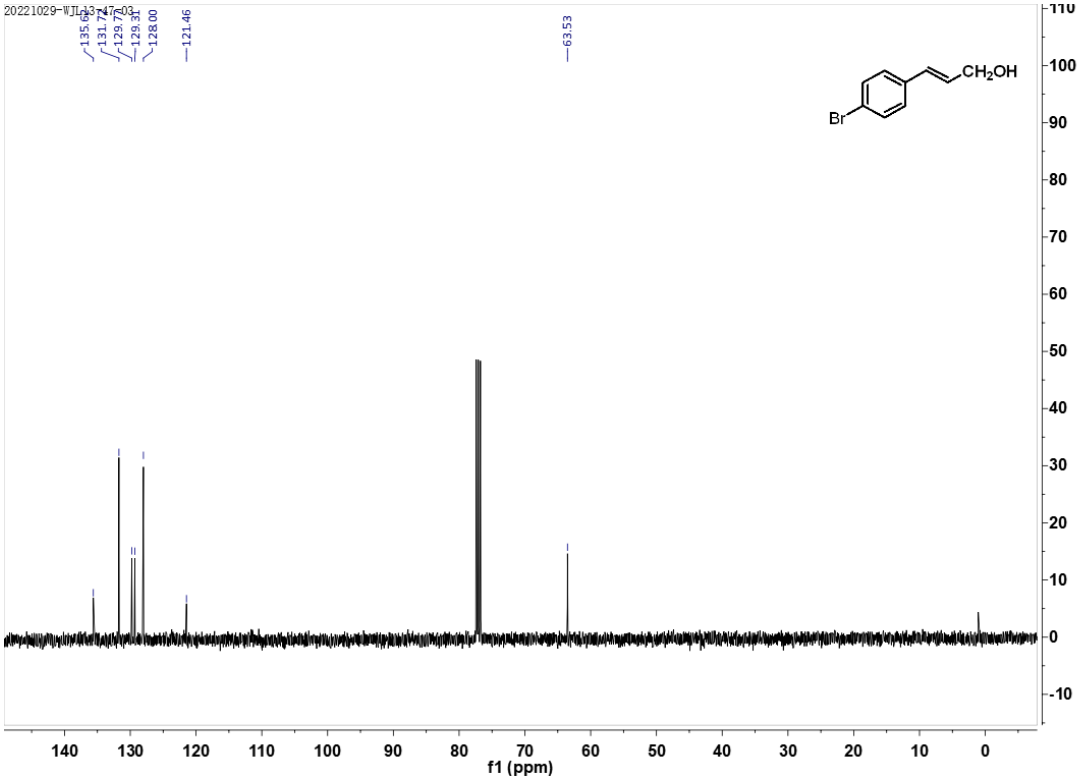

(*E*)-3-(p-tolyl)prop-2-en-1-ol

^{1}H NMR

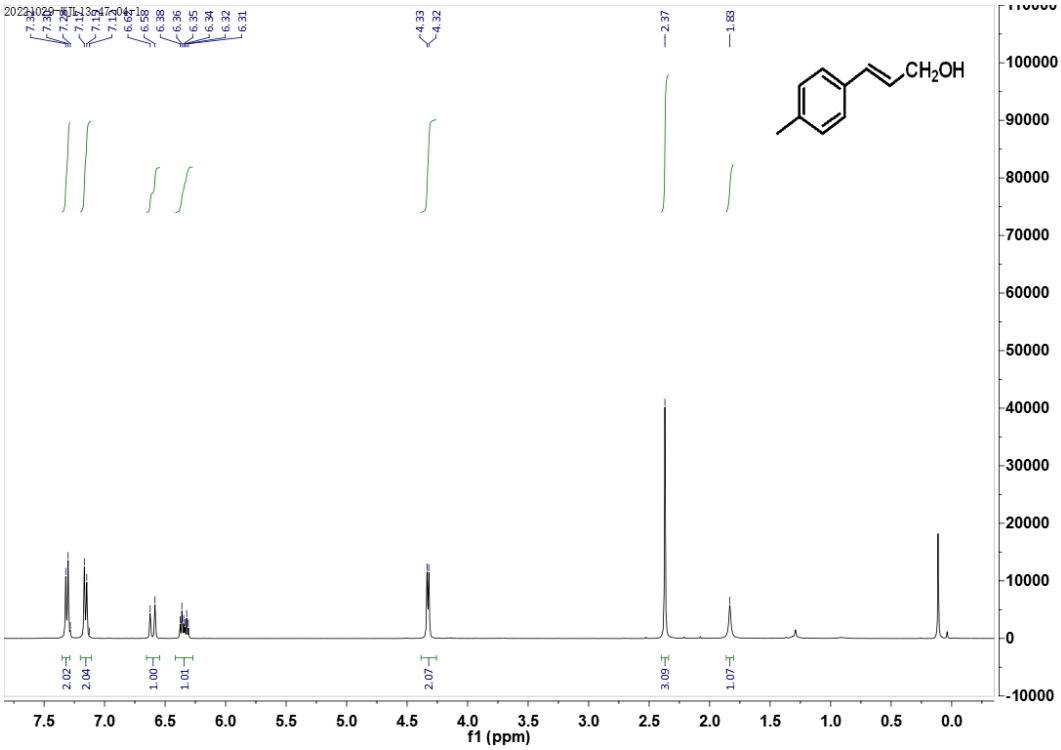

^{13}C NMR

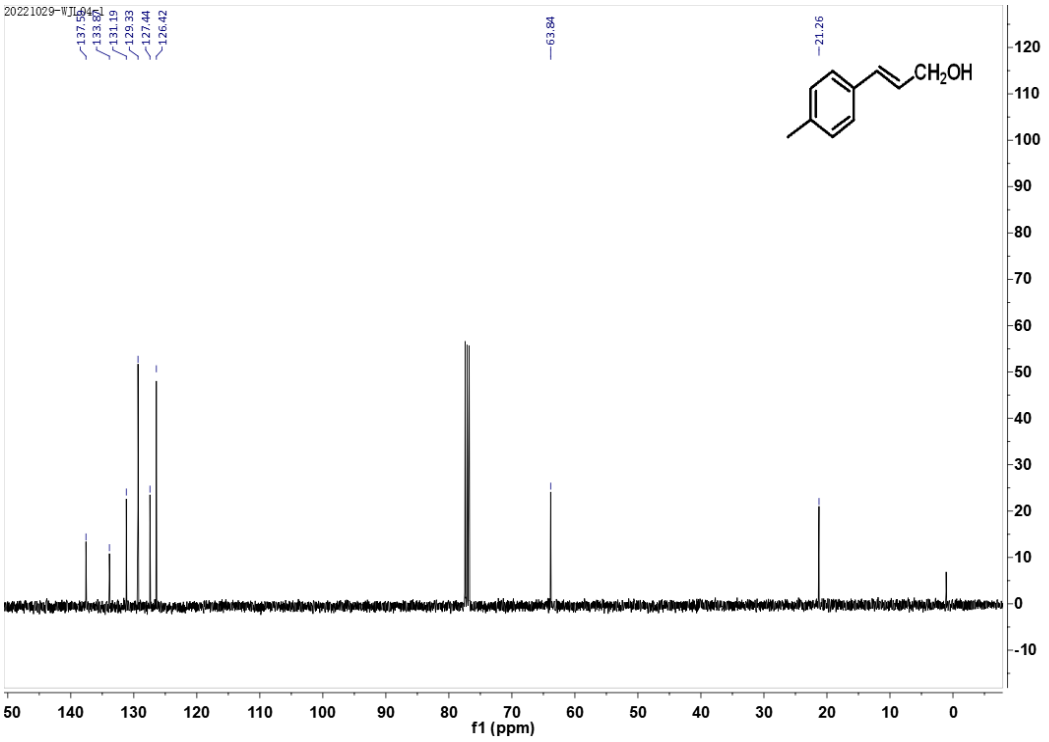

3-phenylprop-2-yn-1-ol

^{1}H NMR

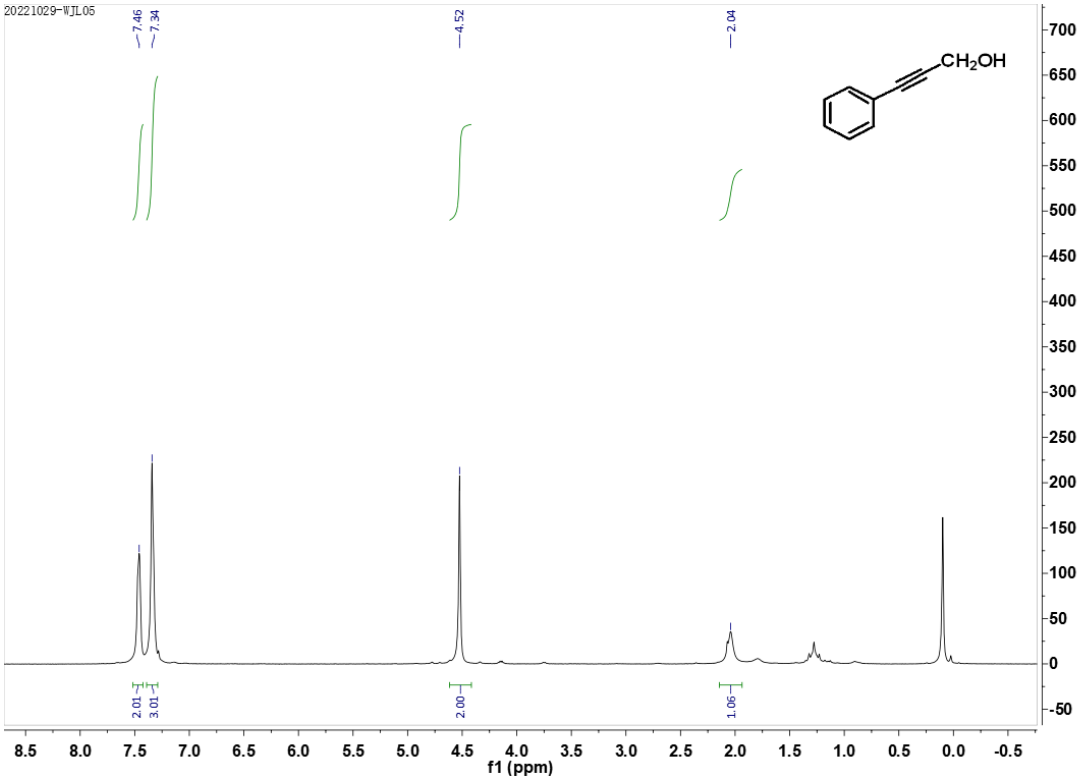

^{13}C NMR

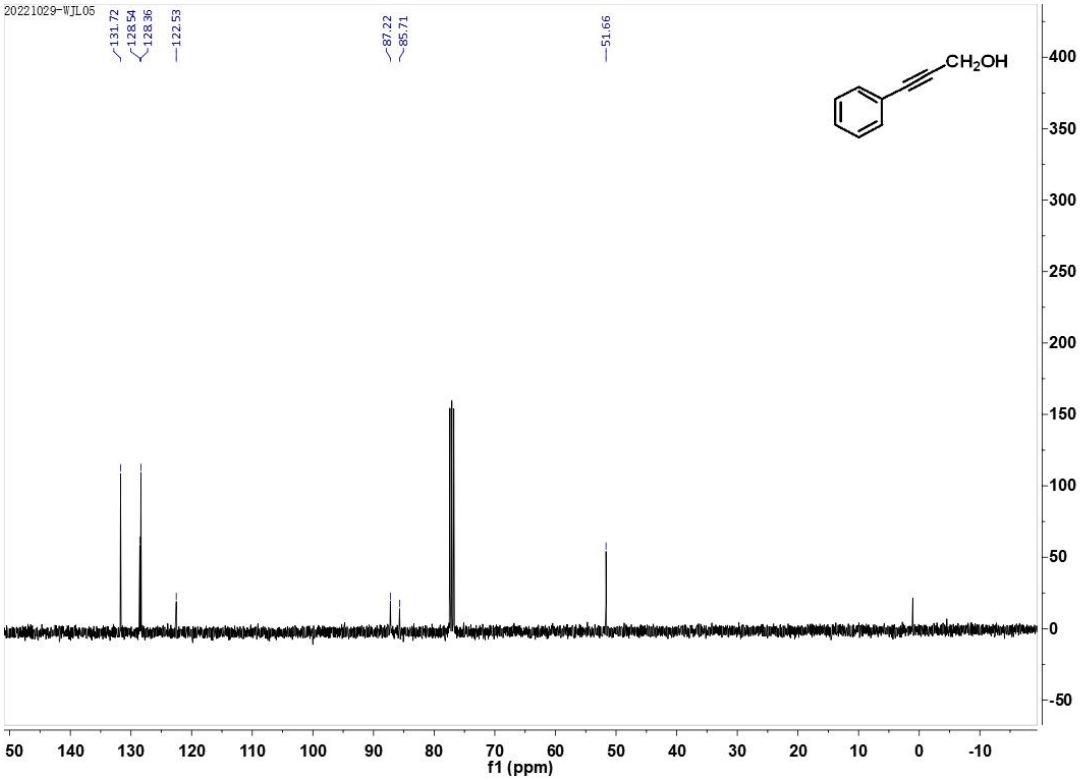

Omega-Undecylenyl alcohol

^{1}H NMR

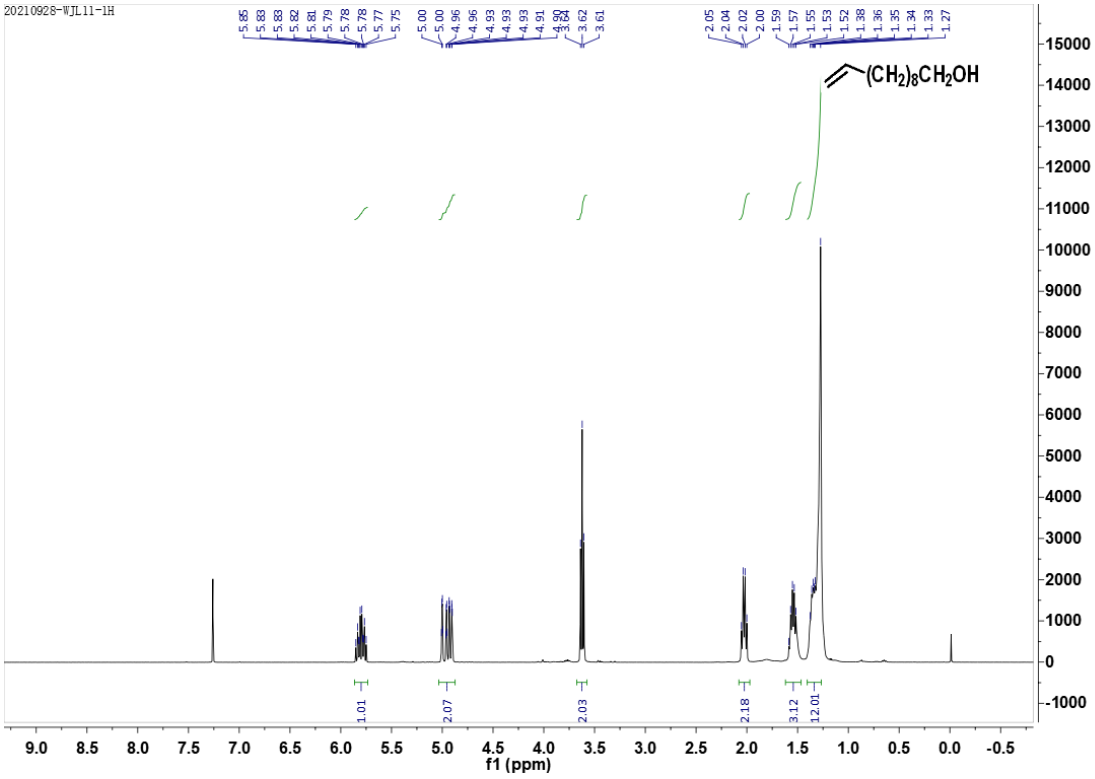

^{13}C NMR

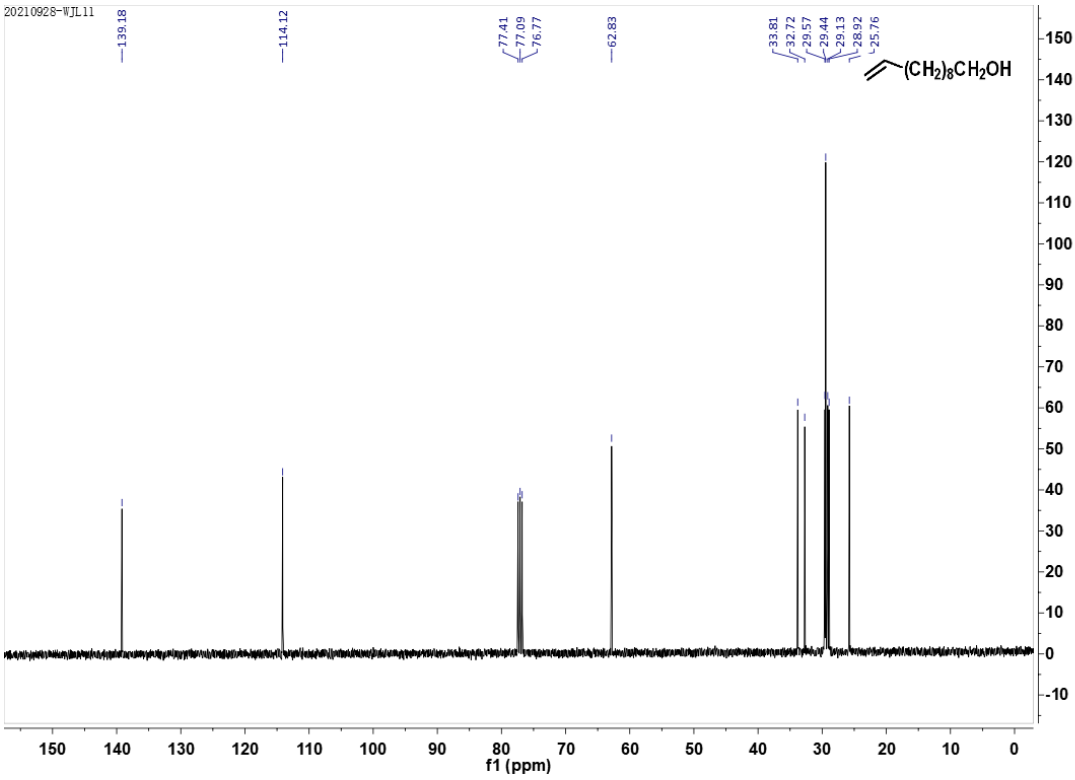

(4-ethynylphenyl)methanol

^{1}H NMR

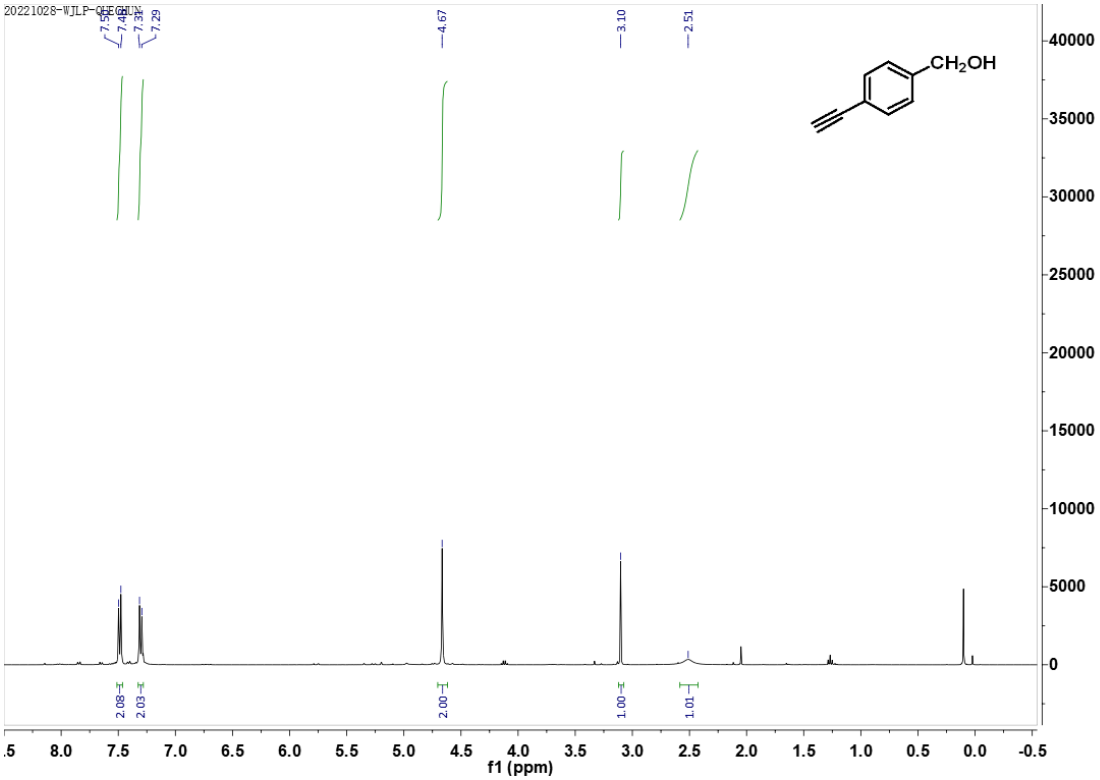

^{13}C NMR

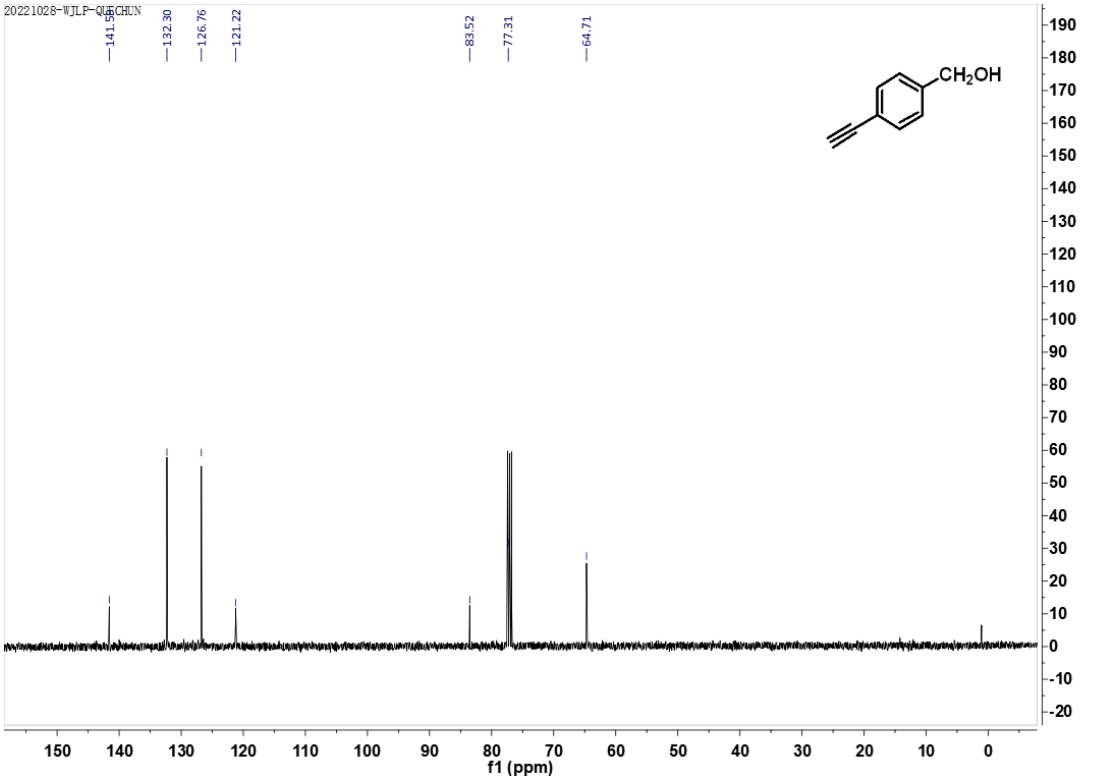

(4-chlorophenyl)methanol

^{1}H NMR

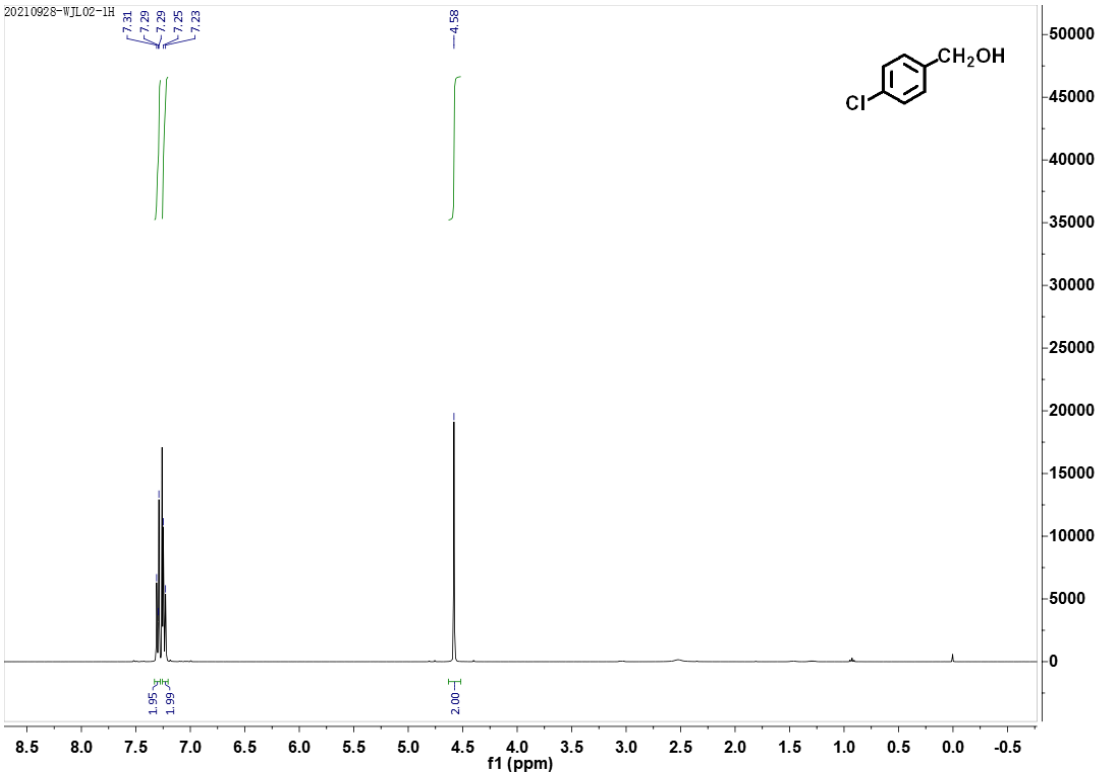

^{13}C NMR

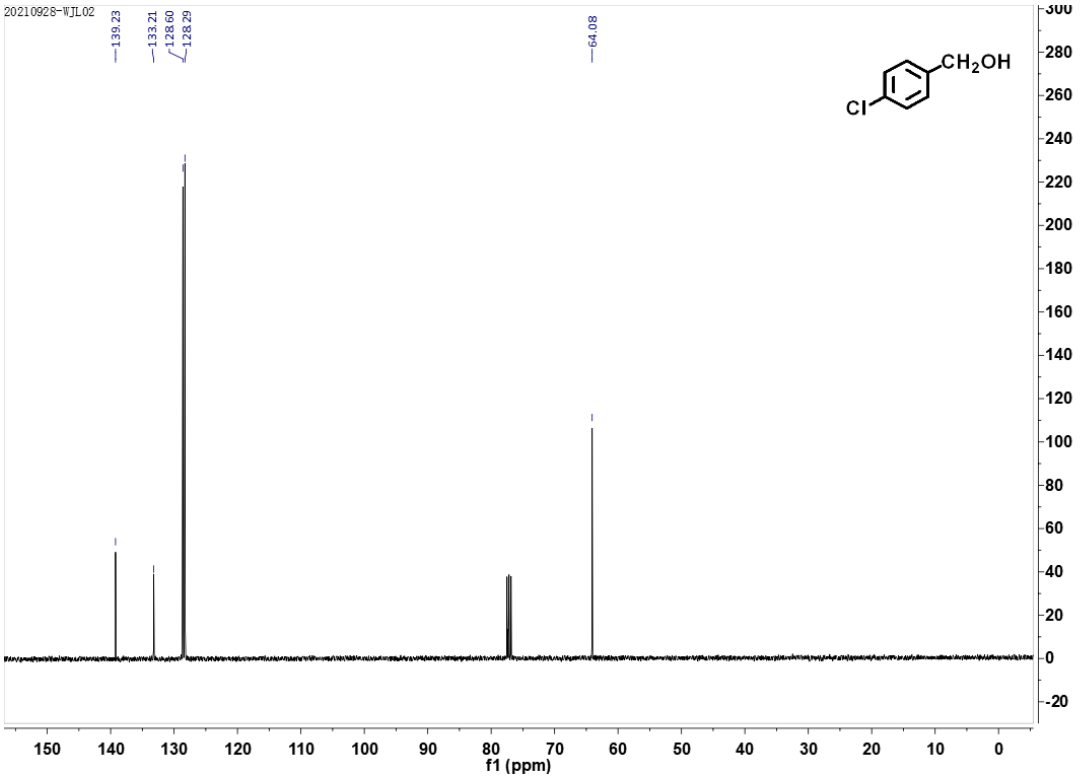

(4-bromophenyl)methanol

^{1}H NMR

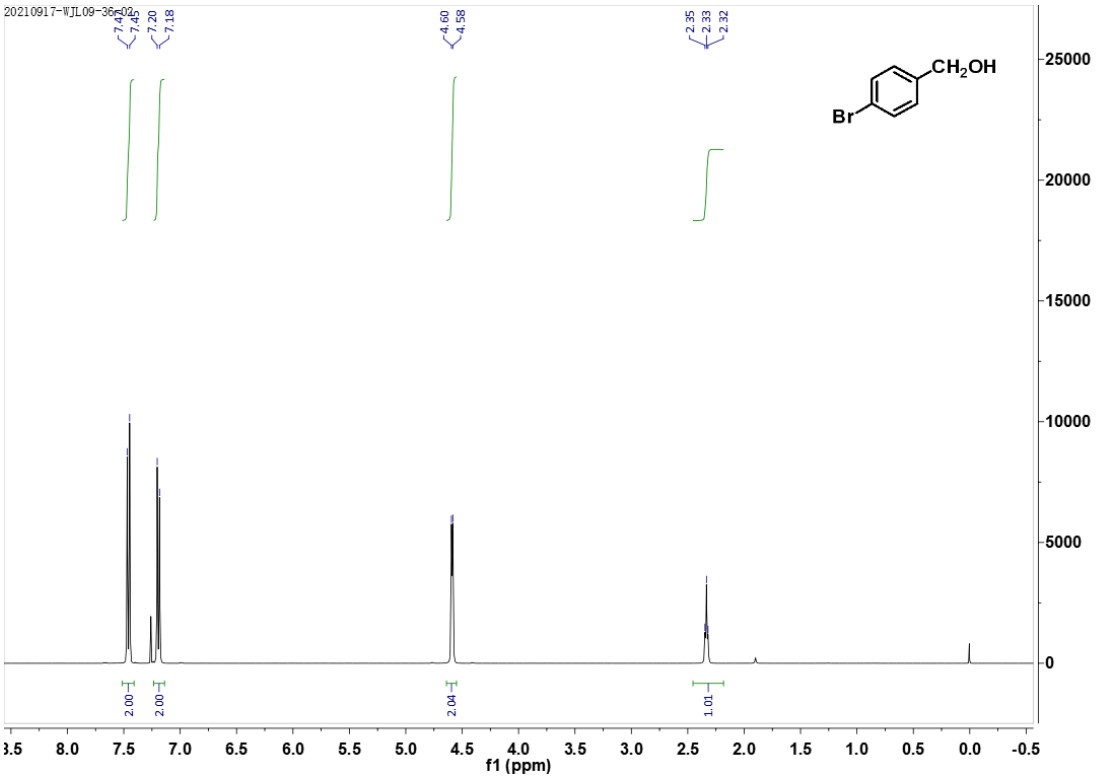

^{13}C NMR

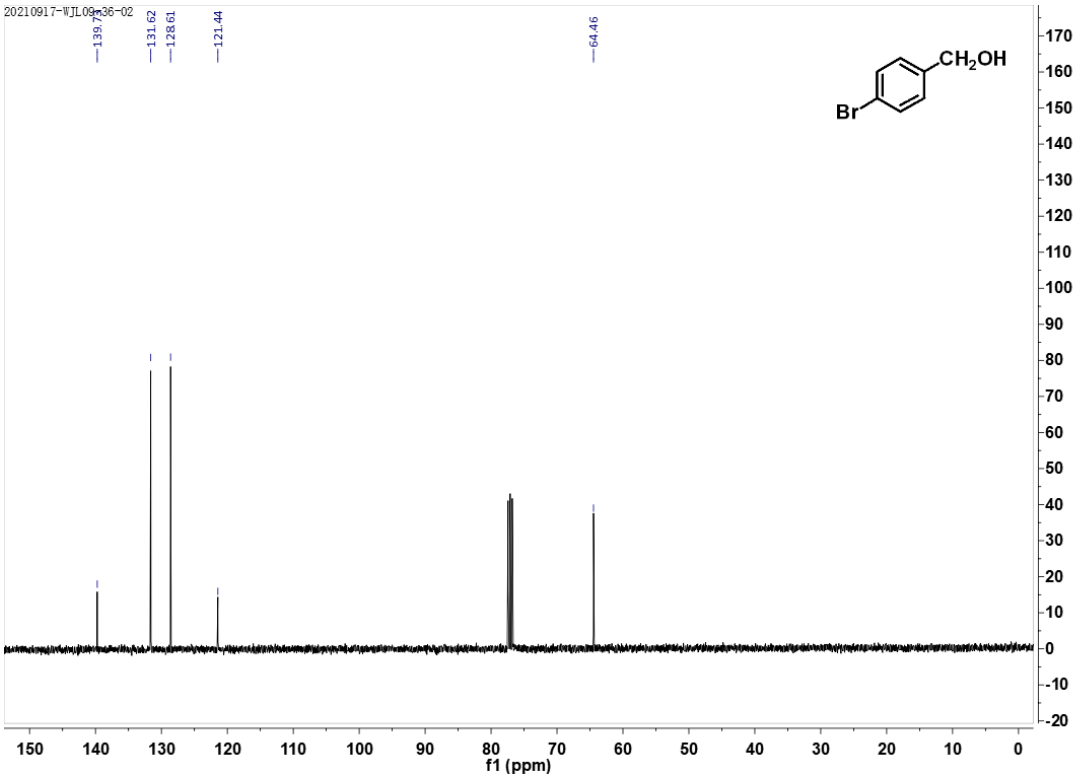

(4-nitrophenyl)methanol

^{1}H NMR

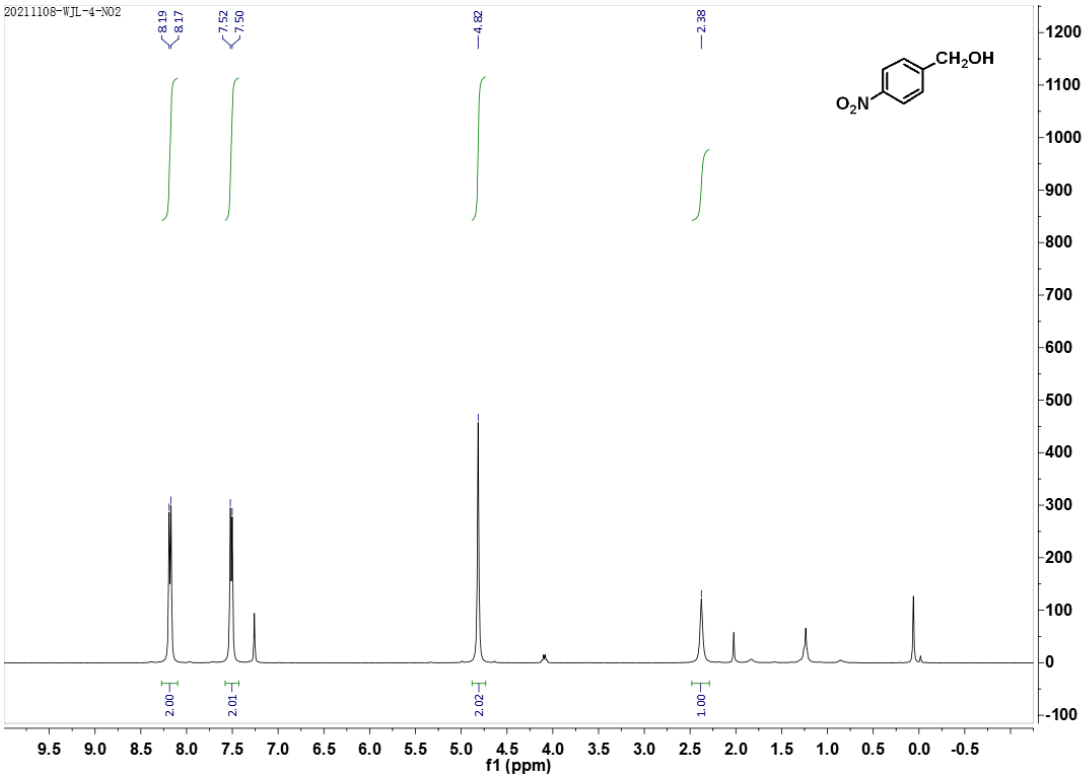

^{13}C NMR

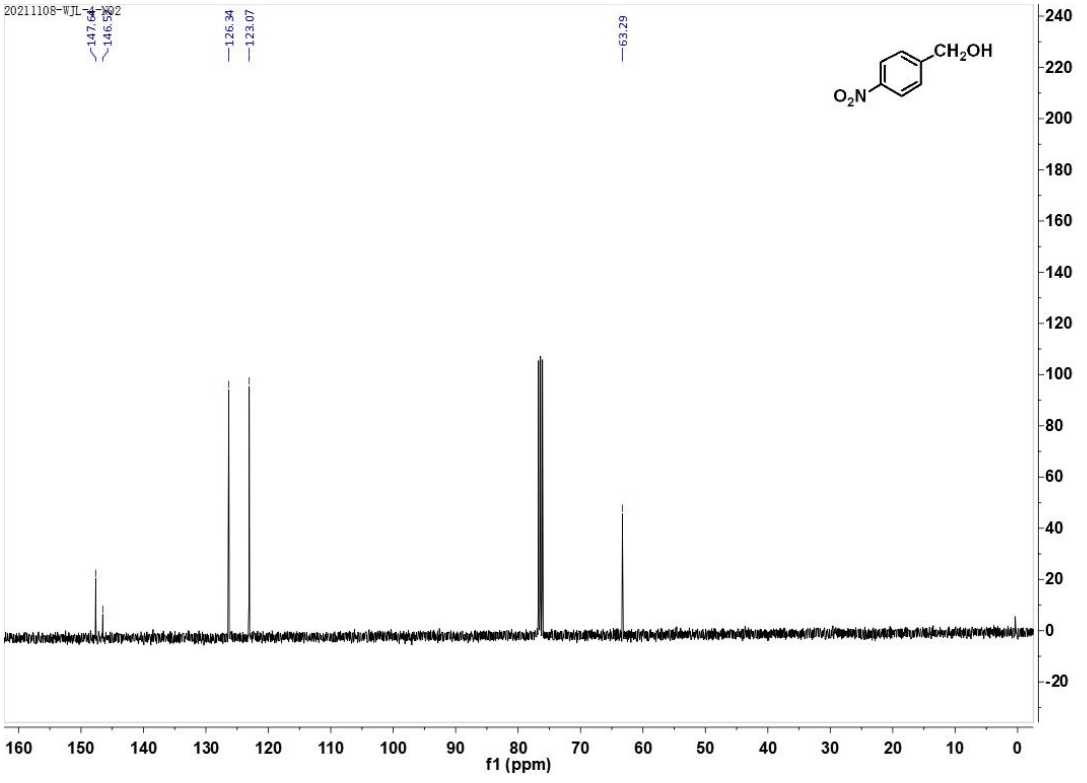

(3-chlorophenyl)methanol

^{1}H NMR

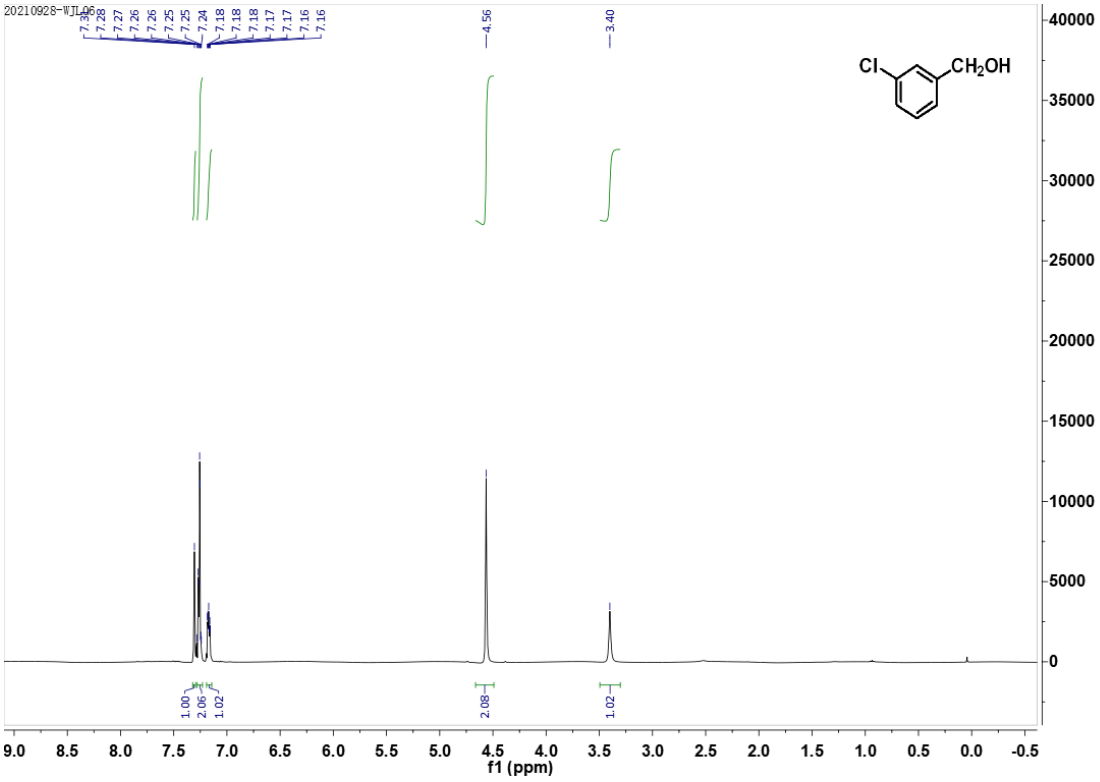

^{13}C NMR

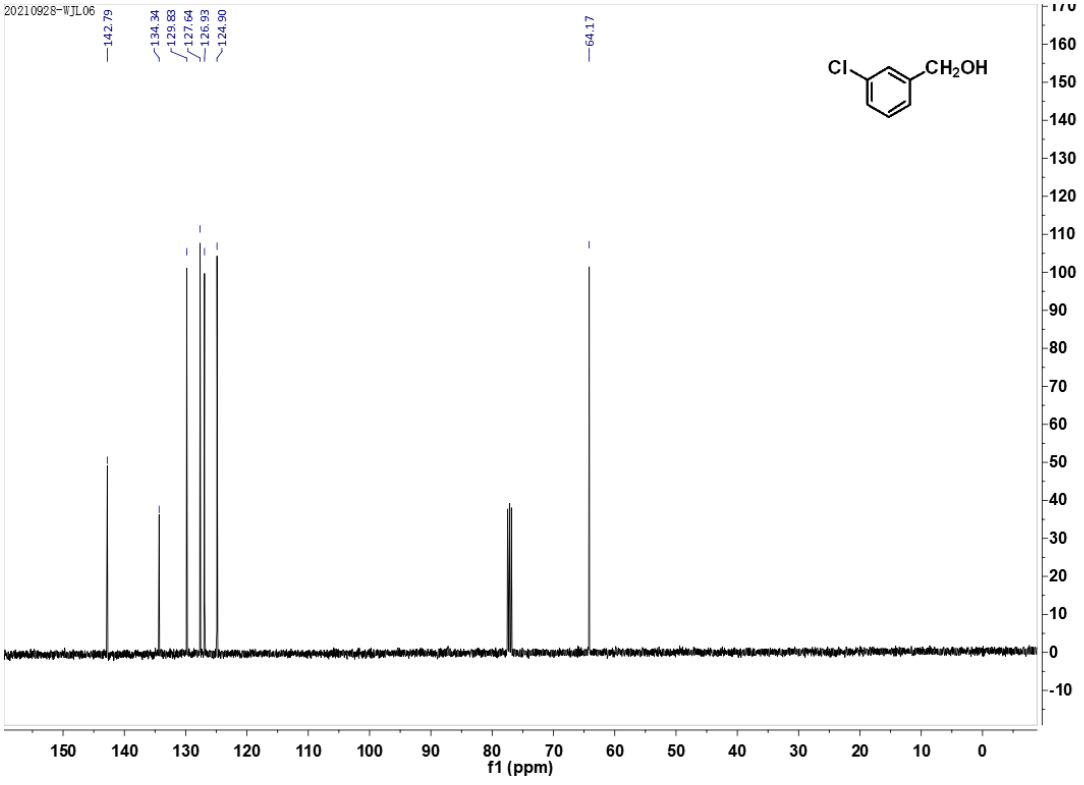

(2-chlorophenyl)methanol

^{1}H NMR

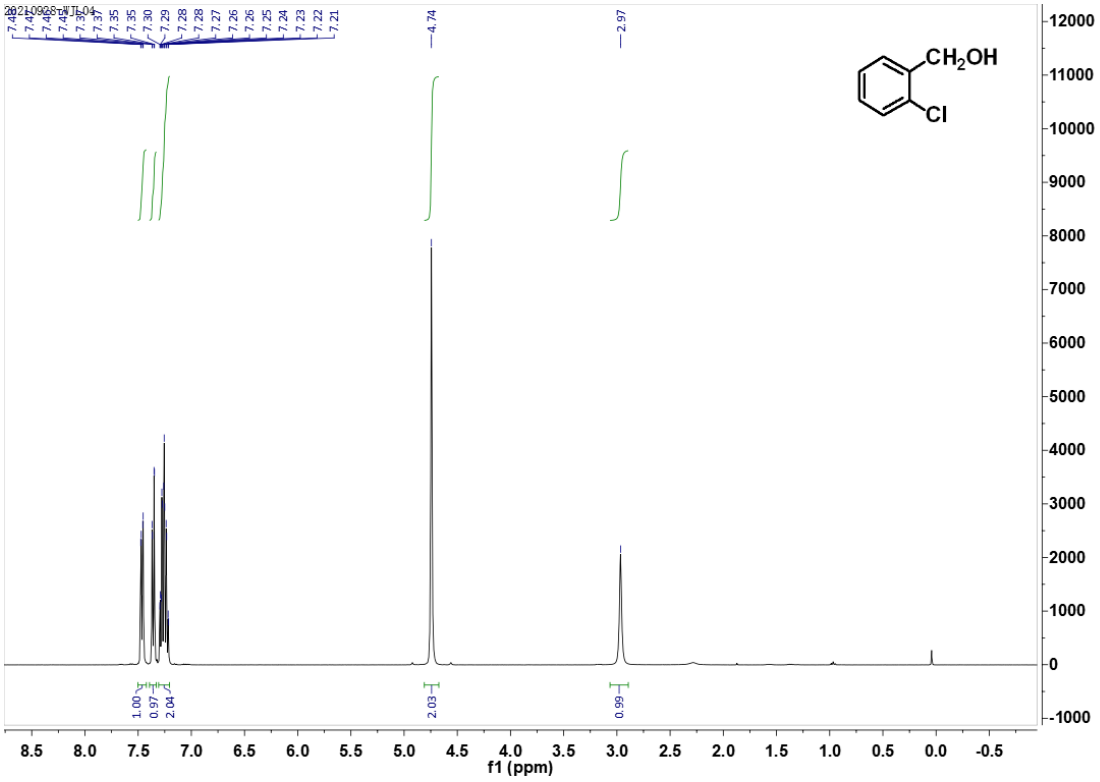

^{13}C NMR

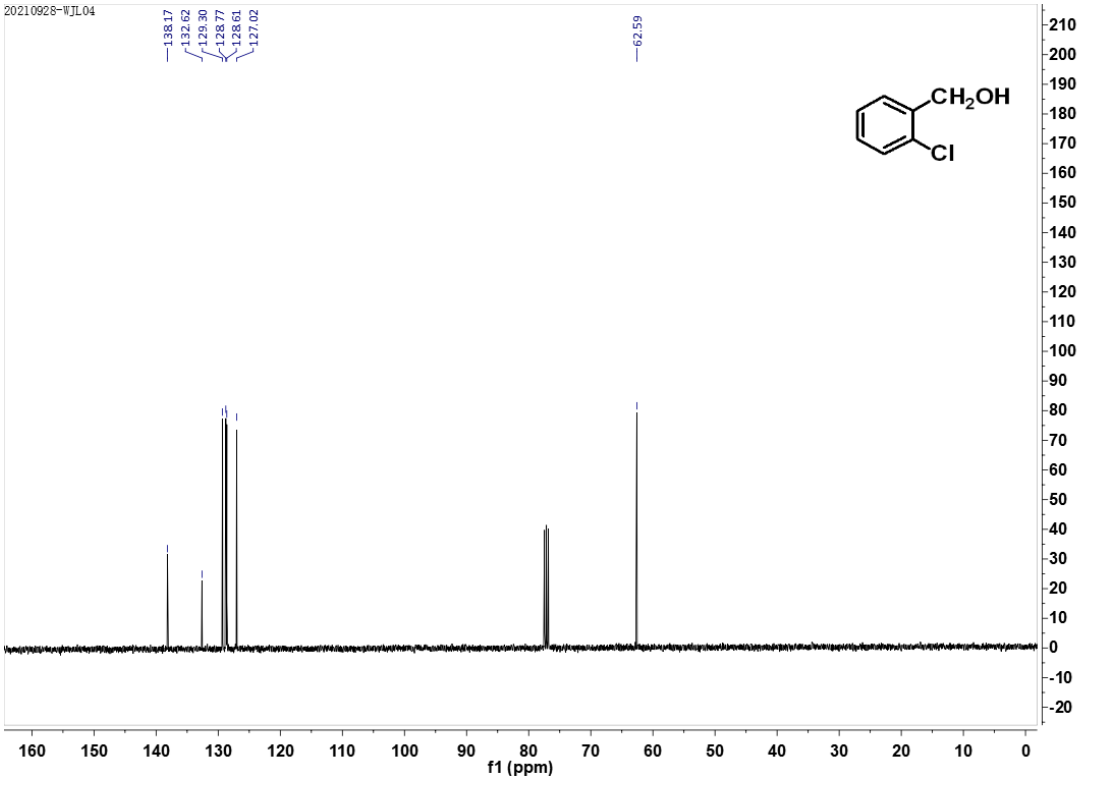

(3a*S*,6a*R*)-1,3-dibenzyltetrahydro-1*H*-furo[3,4-*d*]imidazole-2,4-dione

^{1}H NMR

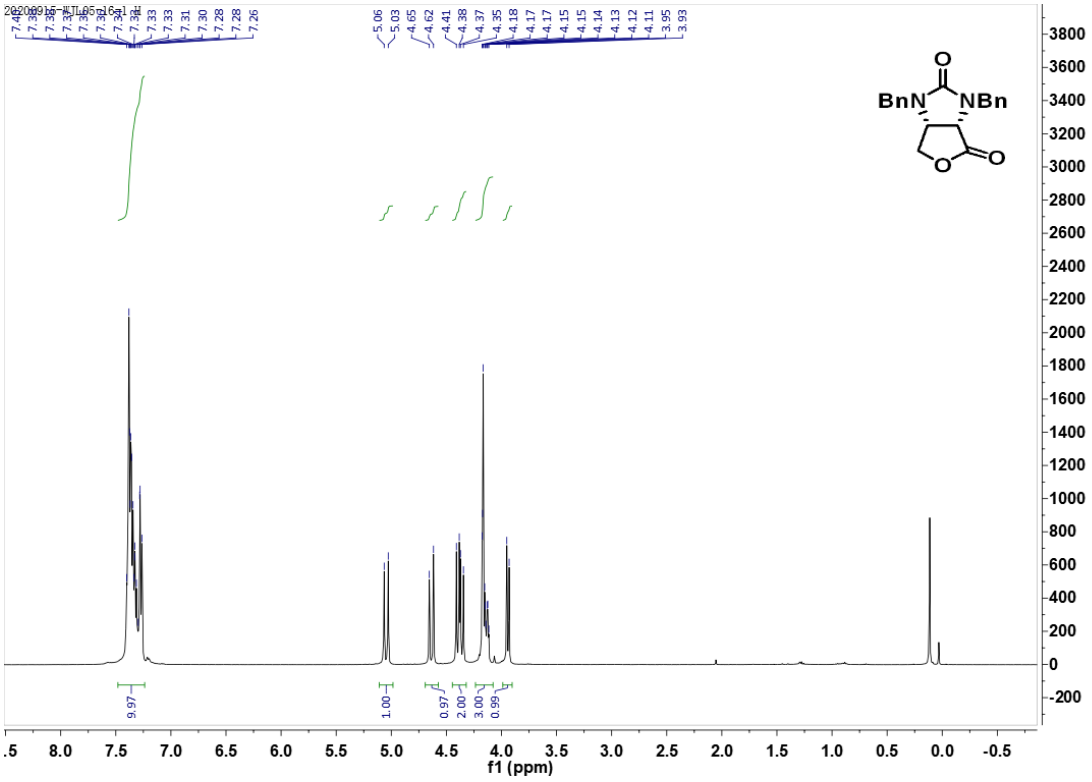

^{13}C NMR

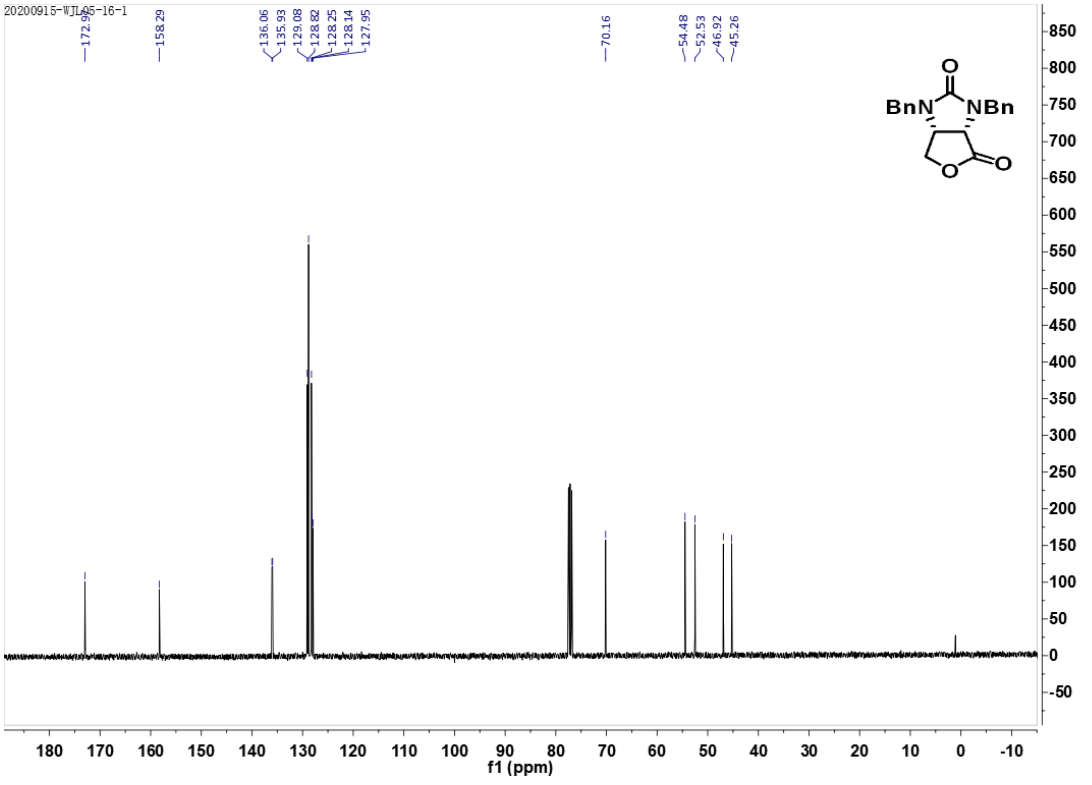

12 References

[1] F. Xiong, X.-X. Chen and F.-E. Chen, *Tetrahedron: Asymmetry*, 2010, **21**, 665-669.

[2] X.-X. Chen, F. Xiong, H. Fu, Z.-Q. Liu and F.-E. Chen, *Chemical and Pharmaceutical Bulletin*, 2011, **59**, 488-491.

[3] H.-F. Dai, W.-X. Chen, L. Zhao, F. Xiong, H. Sheng and F.-E. Chen, *Advanced Synthesis & Catalysis*, 2008, **350**, 1635-1641.

[4] H. C. Brown, Y. M. Choi and S. Narasimhan, *Inorganic Chemistry*, 1981, **20**, 4454-4456.

[5] C. Hu, Z. Huang, M. Jiang, Y. Tao, Z. Li, X. Wu, D. Cheng and F. E. Chen, *ACS Sustainable Chemistry & Engineering*, 2021, **9**, 8990-9000.

[6] D. J. C. Constable, A. D. Curzons and V. L. Cunningham, *Green Chemistry*, 2002, **4**, 521-527.

[7] C. R. McElroy, A. Constantinou, L. C. Jones, L. Summerton and J. H. Clark, *Green Chemistry*, 2015, **17**, 3111-3121.